Explicit-filtering large-eddy simulation using the tensor-diffusivity model supplemented by a dynamic Smagorinsky term

Grégoire S. Winckelmans[a)]
Centre for Systems Engineering and Applied Mechanics (CESAME), Mechanical Engineering Department, Université Catholique de Louvain (UCL), Louvain-la-Neuve 1348, Belgium

Alan A. Wray[b)]
NASA Ames Research Center, Moffet Field, California 94035

Oleg V. Vasilyev[c)]
Mechanical and Aerospace Engineering, University of Missouri–Columbia, Columbia, Missouri 65211

Hervé Jeanmart[d)]
Centre for Systems Engineering and Applied Mechanics (CESAME), Mechanical Engineering Department, Université Catholique de Louvain (UCL), Louvain-la-Neuve 1348, Belgium

(Received 24 April 2000; accepted 9 February 2001)

Large-eddy simulation (LES) with regular explicit filtering is investigated. The filtered-scale stress due to the explicit filtering is here partially reconstructed using the tensor-diffusivity model: It provides for backscatter along the stretching direction(s), and for global dissipation, both also attributes of the exact filtered-scale stress. The necessary LES truncations (grid and numerical method) are responsible for an additional subgrid-scale stress. A natural mixed model is then the tensor-diffusivity model supplemented by a dynamic Smagorinsky term. This model is reviewed, together with useful connections to other models, and is tested against direct numerical simulation (DNS) of turbulent isotropic decay starting with $\mathrm{Re}_\lambda=90$ (thus moderate Reynolds number): LES started from a 256^3 DNS truncated to 64^3 and Gaussian filtered. The tensor-diffusivity part is first tested alone; the mixed model is tested next. Diagnostics include energy decay, enstrophy decay, and energy spectra. After an initial transient of the dynamic procedure (observed with all models), the mixed model is found to produce good results. However, despite expectations based on favorable *a priori* tests, the results are similar to those obtained when using the dynamic Smagorinsky model alone in LES without explicit filtering. Nevertheless, the dynamic mixed model appears as a good compromise between partial reconstruction of the filtered-scale stress and modeling of the truncations effects (incomplete reconstruction and subgrid-scale effects). More challenging 48^3 LES are also done: Again, the results of both approaches are found to be similar. The dynamic mixed model is also tested on the turbulent channel flow at $\mathrm{Re}_\tau=395$. The tensor-diffusivity part must be damped close to the wall in order to avoid instabilities. Diagnostics are mean profiles of velocity, stress, dissipation, and reconstructed Reynolds stresses. The velocity profile obtained using the damped dynamic mixed model is slightly better than that obtained using the dynamic Smagorinsky model without explicit filtering. The damping used so far is however crude, and this calls for further work. © *2001 American Institute of Physics.*
[DOI: 10.1063/1.1360192]

I. INTRODUCTION

This paper is devoted to the investigation of the mixed model formed of the *tensor-diffusivity* model supplemented by a *dynamic Smagorinsky term*. Some preliminary work started with Ref. 1 (also reported, in part, in Ref. 2); it was substantially improved and corrected for the present paper. Thus, we consider large-eddy simulation (LES) of turbulent flows with *explicit filtering*: in addition to the *implicit filtering* due to the effective truncations (grid and numerical method), a regular explicit filter is also assumed, of prescribed shape and effective width larger than the grid spacing. The *filtered-scale* stress due to the explicit filtering is here partially reconstructed using the *tensor-diffusivity* model of Leonard.[3] This model is generic: For all regular symmetric filters that have a nonzero second moment (e.g., the tophat, the Gaussian, most discrete filters), it is found as the first term of the reconstruction series for the filtered-scale stress. As to the dynamic Smagorinsky term, it is used for modeling of the truncation effects: *subgrid-scale* stress and incomplete reconstruction of the filtered-scale stress. This mixed model has already been used by Vreman *et al.*[4,5] with good success. They referred to it as a *dynamic version of the mixed Clark model*. We prefer *tensor-diffusivity model*

[a)]Electronic mail: gsw@term.ucl.ac.be
[b)]Electronic mail: wray@nas.nasa.gov
[c)]Electronic mail: vasilyevo@missouri.edu
[d)]Electronic mail: jeanmart@term.ucl.ac.be

 © 2001 American Institute of Physics

Downloaded 10 May 2001 to 128.206.16.97. Redistribution subject to AIP license or copyright, see http://ojps.aip.org/phf/phfcr.jsp

supplemented by a dynamic Smagorinsky term, as the important tensor-diffusivity part of the model was already proposed by Leonard back in 1974.[3]

Section II is devoted to definitions. In Sec. III, we review theoretical results on direct reconstruction series for the filtered-scale stress, leading to the tensor-diffusivity model. Because of the truncations, the need for a mixed model is identified: We here use the tensor-diffusivity model supplemented by a dynamic Smagorinsky term. This model is reviewed theoretically in Sec. IV and useful connections are made with other models in Sec. V. The dynamic procedure applied to the mixed model is developed in Sec. VI. Results for LES of isotropic turbulent decay started from a direct numerical simulation (DNS) (thus at at moderate Reynolds number: $\mathrm{Re}_\lambda=90$) are then presented in Sec. VII: *a priori* tests and LES runs using the tensor-diffusivity model alone, the dynamic Smagorinsky model alone, and the dynamic mixed model. Comparisons are made with the DNS and with the results of classical LES: LES without explicit filtering, and using the dynamic Smagorinsky model. LES results for the turbulent channel flow at $\mathrm{Re}_\tau=395$ are then presented in Sec. VIII: dynamic mixed model (damped in the wall region) and dynamic Smagorinsky model (also without explicit filtering). Conclusions are provided in Sec. IX, together with the identification of some remaining issues and further work.

II. DEFINITIONS, FILTERED-SCALE STRESS, AND SUBGRID-SCALE STRESS

We consider incompressible turbulent flows ($\partial_k u_k=0$) of Newtonian fluids with constant physical properties. The Navier–Stokes (NS) equations are then

$$\partial_t u_i+\partial_j(u_i u_j)=-\partial_i P+\partial_j(2\nu S_{ij})=-\partial_i P+\nu\,\partial_j\partial_j u_i \tag{1}$$

with $P\overset{\text{def}}{=}p/\rho$ the reduced pressure, ν the kinematic viscosity, and $S_{ij}\overset{\text{def}}{=}(\partial_j u_i+\partial_i u_j)/2$ the strain rate tensor.

Consider an explicit regular filter, $\overline{G}$, applied to a function f. The filtered function, $\overline{f}$, corresponds to a convolution:

$$\overline{f}\overset{\text{def}}{=}\overline{G}*f,\quad \overline{f}(\mathbf{x})\overset{\text{def}}{=}\int \overline{G}(\mathbf{x}-\mathbf{y})\,f(\mathbf{y})\,d\mathbf{y}. \tag{2}$$

We here consider symmetric filters that have a Fourier transform [noted $\overline{\mathcal{G}}(k)$] and a nonzero second moment. Filters for multiple dimensions can be constructed as products of one-dimensional (1-D) filters (this is not the only way but it is the way considered here). Considering first 1-D filters, the filter width, $\overline{\Delta}$, is here normalized using

$$\frac{\overline{\Delta}_c^2}{12}\overset{\text{def}}{=}\overline{\Delta}^2\overset{\text{def}}{=}\int_{-\infty}^{\infty}x^2\,\overline{G}(x)\,dx=-\left.\frac{d^2\overline{\mathcal{G}}}{dk^2}\right|_{k=0}, \tag{3}$$

with $\overline{\Delta}_c$ the *effective width* [based on the top hat filter normalized as $\sin(k\overline{\Delta}_c/2)/(k\overline{\Delta}_c/2)$]. In Fourier space, the filters considered are of the form

$$\overline{\mathcal{G}}(k)=1-\frac{k^2\overline{\Delta}^2}{2}+\ldots, \tag{4}$$

which implies the useful relation

$$\overline{f}=f+\frac{\overline{\Delta}^2}{2}\partial_k\partial_k f+\cdots. \tag{5}$$

Upon applying the $\overline{G}$ filter to the NS equations, one obtains the equation for the filtered field (with $\partial_k\overline{u}_k=0$):

$$\partial_t\overline{u}_i+\partial_j(\overline{u}_i\overline{u}_j)=-\partial_i\overline{P}+\nu\,\partial_j\partial_j\overline{u}_i-\partial_j\tau_{ij}, \tag{6}$$

with τ_{ij} the *filtered-scale* stress which corresponds to the commutator, $\mathcal{K}$, between the operators *product* and *explicit filtering* acting on the field u_i:

$$\tau_{ij}\overset{\text{def}}{=}\overline{u_i u_j}-\overline{u}_i\overline{u}_j\overset{\text{def}}{=}\mathcal{K}(u_i,u_j). \tag{7}$$

So far, Eq. (6) holds independently of any discretization (i.e., no LES since no loss of information). In LES, a significant *truncation filter* is also present: the effective filter due to the LES grid and numerical method. Defining $\tilde{f}$ as the ''LES restricted f'' (i.e., the ''LES resolved f''), we see that what is solved in LES with explicit filtering (which, of course, requires that $\overline{\Delta}_c$ be greater than the grid size Δ) is (view A)

$$\partial_t\tilde{\bar{u}}_i+\partial_j\widetilde{(\tilde{\bar{u}}_i\tilde{\bar{u}}_j)}=-\partial_i\tilde{\bar{P}}+\nu\,\partial_j\partial_j\tilde{\bar{u}}_i-\partial_j\tilde{\mathcal{T}}_{ij}, \tag{8}$$

where the effective stress, $\tilde{\mathcal{T}}_{ij}$, is the LES restriction of $\mathcal{T}_{ij}=\overline{u_i u_j}-\tilde{\bar{u}}_i\tilde{\bar{u}}_j$, which, in turn, can be decomposed as

$$\begin{aligned}\mathcal{T}_{ij}&=\overline{u_i u_j}-\tilde{\bar{u}}_i\tilde{\bar{u}}_j=(\overline{u_i u_j}-\overline{u}_i\overline{u}_j)+(\overline{u}_i\overline{u}_j-\tilde{\bar{u}}_i\tilde{\bar{u}}_j)\\&=\mathcal{K}(u_i,u_j)+\mathcal{H}(\overline{u}_i,\overline{u}_j)\overset{\text{def}}{=}\tau_{ij}+\mathcal{D}_{ij}.\end{aligned} \tag{9}$$

The filtered-scale stress, τ_{ij}, has thus been augmented by an effective *subgrid-scale stress* due to truncation of the filtered field: $\mathcal{D}_{ij}=\mathcal{H}(\overline{u}_i,\overline{u}_j)$ [with $\mathcal{H}(a,b)\overset{\text{def}}{=}\overline{a\,b}-\tilde{\bar{a}}\,\tilde{\bar{b}}$ the fundamental *subgrid-scale operator*: product of complete DNS fields minus product of incomplete LES fields]. Another view (view B) is to consider that what is solved is[6]

$$\partial_t\tilde{\bar{u}}_i+\partial_j\widetilde{(\tilde{\bar{u}}_i\tilde{\bar{u}}_j)}=-\partial_i\tilde{\bar{P}}+\nu\,\partial_j\partial_j\tilde{\bar{u}}_i-\partial_j\tilde{\mathcal{T}}_{ij}. \tag{10}$$

The two views are basically equivalent. Equations (8) and (10) are identical when the regular and truncation filters commute exactly: the case of pseudospectral methods with dealiasing, as the truncation filter is then the sharp Fourier cutoff. Assuming, in what follows, that the two filters ''essentially commute'' in most cases (thus $\overline{\Delta}_c$ is properly chosen with respect to Δ and the numerical method), $\mathcal{T}_{ij}$ is also decomposed as[6]

$$\begin{aligned}\mathcal{T}_{ij}&=\overline{u_i u_j}-\tilde{\bar{u}}_i\tilde{\bar{u}}_j=(\overline{\tilde{\bar{u}}_i\tilde{\bar{u}}_j}-\tilde{\bar{u}}_i\tilde{\bar{u}}_j)+(\overline{u_i u_j-\tilde{\bar{u}}_i\tilde{\bar{u}}_j})\\&=\mathcal{K}(\tilde{\bar{u}}_i,\tilde{\bar{u}}_j)+\overline{\mathcal{H}}(u_i,u_j)\overset{\text{def}}{=}\mathcal{B}_{ij}+\overline{\mathcal{A}}_{ij}.\end{aligned} \tag{11}$$

The stress $\mathcal{B}_{ij}$ is the commutator acting on the discretized field $\tilde{\bar{u}}_i$: it can be reconstructed, as we shall see. The stress $\overline{\mathcal{A}}_{ij}$ corresponds to explicit filtering of $\mathcal{A}_{ij}\overset{\text{def}}{=}\mathcal{H}(u_i,u_j)=u_i u_j-\tilde{\bar{u}}_i\tilde{\bar{u}}_j$: it must be modeled. Thus, in both views, the effective stress is the sum of a *filtered-scale stress* and a *subgrid-scale stress*:

Downloaded 10 May 2001 to 128.206.16.97. Redistribution subject to AIP license or copyright, see http://ojps.aip.org/phf/phfcr.jsp

$$\tilde{\mathcal{T}}_{ij}=\tilde{\tau}_{ij}+\tilde{\mathcal{D}}_{ij}=\tilde{\mathcal{B}}_{ij}+\widetilde{\overline{\mathcal{A}}_{ij}}=\tilde{\mathcal{B}}_{ij}+\bar{\mathcal{A}}_{ij}. \tag{12}$$

How does all this relate to ''classical LES'' without explicit filtering? In that case, the only filtering is the one due to the effective truncations. What is solved is then

$$\partial_t\tilde{u}_i+\partial_j\widetilde{(\tilde{u}_i\tilde{u}_j)}=-\partial_i\tilde{P}+\nu\,\partial_j\partial_j\tilde{u}_i-\partial_j\tilde{\mathcal{A}}_{ij}. \tag{13}$$

The effective stress, $\tilde{\mathcal{A}}_{ij}=\tilde{\mathcal{H}}(u_i,u_j)=\widetilde{u_iu_j}-\widetilde{\tilde{u}_i\tilde{u}_j}$, is a pure subgrid-scale stress: it must be modeled. Using the decomposition of Eq. (11), it is easily seen that Eq. (10) corresponds to explicit filtering of Eq. (13). LES with explicit filtering corresponds to a ''change of basis:'' work using the $\bar{\tilde{u}}_i$ basis instead of the $\tilde{u}_i$ basis, with the hope that reconstruction/modeling of the effective stress in the new basis might be easier and lead to better results.

III. RECONSTRUCTION, TENSOR-DIFFUSIVITY MODEL, AND MIXED MODEL

We consider nonlinear models of the family derived from Yeo and Bedford[7–9] and Leonard.[3,10] Consider first the Gaussian filter with the normalization of Eq. (3):

$$\overline{G}(x)=\frac{1}{\overline{\Delta}\sqrt{2\pi}}\exp\left(-\frac{x^2}{2\overline{\Delta}^2}\right),\quad \overline{\mathcal{G}}(k)=\exp\left(-\frac{k^2\overline{\Delta}^2}{2}\right). \tag{14}$$

The complete, infinite, reconstruction series is obtained as[8–10]

$$\mathcal{K}(f,g)=\overline{fg}-\overline{f}\,\overline{g}=\overline{\Delta}^2\,\partial_x\overline{f}\partial_x\overline{g}+\frac{\overline{\Delta}^4}{2!}\partial_x\partial_x\overline{f}\partial_x\partial_x\overline{g}+\frac{\overline{\Delta}^6}{3!}\partial_x\partial_x\partial_x\overline{f}\partial_x\partial_x\partial_x\overline{g}+\cdots. \tag{15}$$

This result is remarkable because, at least for the case without additional truncation, it provides a mean for direct reconstruction of the filtered-scale stress using only the filtered field and working only in physical space. In three dimensions, we assume explicit filters that are formed as the product of 1-D symmetric filters, each with uniform filter width, $\overline{\Delta}_k$. (The case of nonuniform filter width is not addressed theoretically in this paper.) One then easily obtains the reconstruction series for the filtered-scale stress:

$$\tau_{ij}=\overline{\Delta}_k^2\,\partial_k\overline{u}_i\,\partial_k\overline{u}_j+\frac{\overline{\Delta}_k^2\overline{\Delta}_l^2}{2!}\partial_k\partial_l\overline{u}_i\partial_k\partial_l\overline{u}_j+\frac{\overline{\Delta}_k^2\overline{\Delta}_l^2\overline{\Delta}_m^2}{3!}\partial_k\partial_l\partial_m\overline{u}_i\partial_k\partial_l\partial_m\overline{u}_j+\ldots, \tag{16}$$

where summation is here assumed over the triply repeated indices. The case where the filter width is the same in all directions corresponds to $\overline{\Delta}_k=\overline{\Delta}$. We notice that the series includes reconstruction of the trace of τ_{ij}. Furthermore, it was recently shown[6,11] that, for all symmetric filters that are C^∞ in Fourier space and that have a nonzero second moment (that is most of the filters defined in physical space, e.g., the Gaussian, the top hat, most discrete filters): (1) one can obtain the infinite reconstruction series (from generating functions), and (2) it always starts with the same first term—the tensor-diffusivity term:

$$\tau_{ij}=\overline{\Delta}_k^2\,\partial_k\overline{u}_i\,\partial_k\overline{u}_j+\cdots. \tag{17}$$

This term is thus generic to all filters that have a Fourier transform starting as Eq. (4).

Of course, the full reconstruction of τ_{ij} requires the complete filtered field, $\overline{u}_i$: This is of little use in LES. What is needed in practical LES is the partial reconstruction of $\tilde{\mathcal{B}}_{ij}$, using only the truncated and filtered field, $\bar{\tilde{u}}_i$.

In all that follows, we further require that $\overline{\mathcal{G}}(k)>0$ for all k significant to the LES $[0\leqslant k\leqslant k_{\max}=(\pi/\Delta)-1]$. This is always feasible (e.g., by properly choosing the explicit filter width, $\overline{\Delta}_c$, in relation to the grid size, Δ). In spectral methods, one could then defilter $\bar{\tilde{u}}_i$ [by using $1/\overline{\mathcal{G}}(k)$] to obtain an approximation to $\tilde{u}_i$. This is true for spectral methods but of little interest to practical LES: Reconstruction must (1) be feasible without defiltering and (2) be feasible in physical space, so that it can be used in finite difference methods, etc. The direct reconstruction series does that

$$\tilde{\mathcal{B}}_{ij}^M=\overline{\Delta}_k^2\,\partial_k\widetilde{\bar{\tilde{u}}_i}\,\partial_k\bar{\tilde{u}}_j+\cdots. \tag{18}$$

(In what follows, the superscript ''M'' always refers to a modeled quantity.)

Another approach is that used by Stolz and Adams:[12] One first reconstructs an approximate $\tilde{u}_i$ from $\bar{\tilde{u}}_i$ using the van Cittert iterative deconvolution method,

$$\tilde{u}_i^M=\bar{\tilde{u}}_i+(I-\overline{G})*\bar{\tilde{u}}_i+(I-\overline{G})*((I-\overline{G})*\bar{\tilde{u}}_i)+\ldots, \tag{19}$$

and one then uses $\tilde{\mathcal{B}}_{ij}^M=\widetilde{\tilde{u}_i^M\tilde{u}_j^M}-\widetilde{\bar{\tilde{u}}_i\bar{\tilde{u}}_j}$. For instance, the lowest level deconvolution gives $\tilde{u}_i^M=2\,\bar{\tilde{u}}_i-\bar{\bar{\tilde{u}}}_i$. For high level deconvolution, the iterative method is more efficient than evaluating the higher order terms in the direct reconstruction series, Eq. (18).

The approach followed here is to use the direct reconstruction series, but to keep only the first, most necessary and generic term: the tensor-diffusivity term. This lowest level reconstruction model (1) can be efficiently evaluated, (2) provides for local backscatter, global dissipation, and is time reversible, these also being attributes of the exact filtered-scale stress, see Refs. 6 and 11. In summary:

(1) The LES grid, Δ, is chosen (with respect to scales corresponding to the inertial range).
(2) The explicit filter is chosen. Its effective width, $\overline{\Delta}_c$, is chosen larger than the grid size, Δ, yet such that $\overline{\mathcal{G}}(k)>0$ for all k relevant to the LES.
(3) The direct reconstruction series, Eq. (18), is truncated to the first and most necessary term. $\overline{\Delta}_c$ must also be such that this term corresponds to significant (yet incomplete) reconstruction of $\tilde{\mathcal{B}}_{ij}$.

The tensor-diffusivity model was first proposed by Leonard.[3] It was tested, *a priori*, against experimental data (unfortunately two-dimensional cuts) in Ref. 13 with stress correlation levels of about 0.7, and against DNS data in Ref.

Downloaded 10 May 2001 to 128.206.16.97. Redistribution subject to AIP license or copyright, see http://ojps.aip.org/phf/phfcr.jsp

14 with correlation levels between 0.83 and 0.97 depending on the type and width of the explicit filter. Our *a priori* tests also showed high correlations (see Sec. VII and Ref. 6). Because of the losses of information (LES truncations and truncation of the reconstruction series), this model does not suffice: The dissipation is far too low. The additional required dissipation corresponds to loss of information (here ''subgrid-scale'' modeling + ''truncated reconstruction'' modeling) and must be provided by an added term: We here use a purely dissipative effective viscosity model. Thus, the practical model for LES with explicit filtering is here of the mixed type, as in Vreman *et al.*:[4,5]

$$\tilde{\mathcal{T}}_{ij}^{M}=\overline{\Delta}_k^2\,\partial_k\widetilde{\bar{\tilde{u}}_i\,\partial_k\bar{\tilde{u}}_j}-2\,\widetilde{\tilde{\nu}_e\bar{\tilde{S}}_{ij}}\,, \tag{20}$$

where $\bar{\tilde{S}}_{ij}$ is the strain rate tensor of the filtered and truncated field, and where $\tilde{\nu}_e$ is an effective viscosity (see also Refs. 6 and 11 for further discussion of the truncation model). Equation (20) is thus what is used here to model the sum of the two terms for $\tilde{\mathcal{T}}_{ij}$, as in Eq. (12). As the truncation model has no contribution to modeling the trace of $\tilde{\mathcal{T}}_{ij}$, the mixed model cannot claim to model the full $\tilde{\mathcal{T}}_{ij}$. What is implied is

$$\tilde{\mathcal{T}}_{ij}^{*\,M}=(\overline{\Delta}_k^2\,\partial_k\widetilde{\bar{\tilde{u}}_i\,\partial_k\bar{\tilde{u}}_j}^{*}-2\,\widetilde{\tilde{\nu}_e\bar{\tilde{S}}_{ij}}\,, \tag{21}$$

where the asterisk (*) stands for the traceless part of a tensor (e.g., $\tilde{\mathcal{T}}_{ij}^{*}\overset{\text{def}}{=}\tilde{\mathcal{T}}_{ij}-\frac{1}{3}\tilde{\mathcal{T}}_{kk}\,\delta_{ij}$, etc., a convention that will be kept throughout).

Following Smagorinsky[15] for LES without explicit filtering and with $\tilde{\nu}_e=C\,\Delta^2\,|\tilde{S}|$ (where $|\tilde{S}|^2\overset{\text{def}}{=}2\,\widetilde{\tilde{S}_{kl}\tilde{S}_{kl}}$), we here use $\tilde{\nu}_e=C\,\Delta^2\,|\bar{\tilde{S}}|$ with C determined through the *dynamic procedure*[16–20] adapted to the mixed model with explicit filtering, see Sec. VI. Thus, classical modeling is followed, but using the filtered field $|\bar{\tilde{S}}|$ and relying on the dynamic procedure to determine the proper C. In practice, we program the mixed model as in Eq. (20),

$$\tilde{\mathcal{T}}_{ij}^{M}=\overline{\Delta}_k^2\,\partial_k\widetilde{\bar{\tilde{u}}_i\,\partial_k\bar{\tilde{u}}_j}-2\,C\,\Delta^2\,\widetilde{|\bar{\tilde{S}}|\bar{\tilde{S}}_{ij}}, \tag{22}$$

but we remain vigilant as far as the trace components are concerned. In terms of dissipation, it does not matter since the trace component has no net contribution.

Other choices than Ref. 15 can be used for the inverse time scale in the effective viscosity, see, e.g., Ref. 21 for a scaling based on enstrophy, and Refs. 22–24 for reviews and *a priori* tests. With the dynamic procedure, the choice of scaling is not that important as the procedure determines the proper C in each case. One can even use a ''Kolmogorov'' scaling,[25] $\tilde{\nu}_e=(C\,\epsilon^{1/3})\,\Delta^{4/3}$, and a dynamic procedure that finds the value for the dimensional product $(C\,\epsilon^{1/3})$, see the results in Ref. 26. We also notice a new scaling based on the square of the velocity gradient tensor,[27] and that allows for wall bounded flows without requiring the dynamic procedure.

Finally, we remain convinced that the development of better truncation models is still required (e.g., anisotropic models as in Ref. 28, multiscale models as in Ref. 29); they must however remain mainly dissipative, as loss of information is not reversible.

IV. THEORETICAL BEHAVIOR OF THE MIXED MODEL

For simplicity, we consider the case where the filter size is the same in all directions:

$$\tilde{\mathcal{T}}_{ij}^{M}=\overline{\Delta}^2\,\partial_k\widetilde{\bar{\tilde{u}}_i\,\partial_k\bar{\tilde{u}}_j}-2\,C\,\Delta^2\,\widetilde{|\bar{\tilde{S}}|\bar{\tilde{S}}_{ij}}. \tag{23}$$

When used as forcing in the LES equations, the first term behaves as a directional diffusion/antidiffusion, hence its name: *tensor-diffusivity* model. Indeed, it is easily seen[10] that

$$-\overline{\Delta}^2\,\partial_j(\partial_k\bar{\tilde{u}}_i\partial_k\bar{\tilde{u}}_j)=-\overline{\Delta}^2\,\bar{\tilde{S}}_{jk}\,\partial_j\partial_k\bar{\tilde{u}}_i\,, \tag{24}$$

so that $\bar{\tilde{S}}_{jk}$ plays the role of a tensorial effective viscosity. Since the tensor $\bar{\tilde{S}}_{jk}$ is not positive definite (as its eigenvalues sum to zero), one has effectively negative diffusion along the stretching direction(s). This part of the mixed model provides naturally for local directional backscatter of energy (as does the exact filtered-scale stress). What about the global dissipation of the filtered and truncated field? We here consider isotropic turbulence: thus, $C=C(t)>0$. Defining $\langle\cdots\rangle$ as the integrated (or mean) value, the molecular viscosity contribution to dissipation is

$$\langle\epsilon^{\nu}\rangle=-\langle\widetilde{\tilde{\tau}_{ij}^{\nu}\bar{\tilde{S}}_{ij}}\rangle=\nu\,\langle\widetilde{2\,\bar{\tilde{S}}_{ij}\bar{\tilde{S}}_{ij}}\rangle=\nu\,\langle\widetilde{\bar{\tilde{\omega}}_i\bar{\tilde{\omega}}_i}\rangle=2\,\nu\,\langle\mathcal{E}\rangle, \tag{25}$$

where $\bar{\tilde{\omega}}_i$ is the vorticity of the field $\bar{\tilde{u}}_i$ and $\langle\mathcal{E}\rangle$ is its global enstrophy. This contribution is positive everywhere. The contribution of the mixed model is[10]

$$\begin{aligned}\langle\epsilon^{M}\rangle&=-\langle\widetilde{\tilde{\mathcal{T}}_{ij}^{*\,M}\bar{\tilde{S}}_{ij}}\rangle\\&=-\langle\widetilde{\tilde{\mathcal{T}}_{ij}^{M}\bar{\tilde{S}}_{ij}}\rangle\\&=-\overline{\Delta}^2\,\langle\widetilde{\widetilde{\partial_k\bar{\tilde{u}}_i\,\partial_k\bar{\tilde{u}}_j}\bar{\tilde{S}}_{ij}}\rangle+C\,\Delta^2\langle\widetilde{2\,|\bar{\tilde{S}}|\,\bar{\tilde{S}}_{ij}\,\bar{\tilde{S}}_{ij}}\rangle.\end{aligned} \tag{26}$$

The Smagorinsky contribution is positive everywhere. The first term contribution is not positive everywhere. Globally however, the first term is proportional to the opposite of the skewness, here defined as

$$\langle\mathcal{S}\rangle=\langle\widetilde{\widetilde{\partial_k\bar{\tilde{u}}_i\,\partial_k\bar{\tilde{u}}_j}\bar{\tilde{S}}_{ij}}\rangle. \tag{27}$$

It is thus positive if the skewness of the LES field is negative. The skewness is negative in isotropic turbulence and its DNS. It is also found to be negative in LES of isotropic turbulence that is started from a filtered and truncated DNS. If, instead, one starts the LES for a random field, the skewness is initially zero but it quickly becomes negative as the flow develops into LES of real turbulence, see, e.g., investigations in Ref. 6.

V. TIES WITH OTHER MODELS

In order to put the tensor-diffusivity model into proper perspective, we identify further relations between this model and previous work in literature. Recall that this model is basically due to Leonard.[3]

The mixed model (20) was not explicitly considered in the models evaluated, *a priori*, by Clark *et al.*,[23] although it

Downloaded 10 May 2001 to 128.206.16.97. Redistribution subject to AIP license or copyright, see http://ojps.aip.org/phf/phfcr.jsp

can be reconstructed from different formulas provided in the paper. The credit should thus also be partially attributed to these authors.

The mixed model was also not considered in the models evaluated, *a priori*, in Ref. 30. These were constructed using all admissible combinations of the strain rate and rotation tensors. We notice, however, that the mixed model corresponds to a judicious combination of the terms considered.

The tensor-diffusivity model is also recalled to have strong ties with the scale-similarity model of Bardina:[31]

$$\tilde{\mathcal{B}}_{ij}^{M}=\widetilde{\bar{\tilde{u}}_i\bar{\tilde{u}}_j}-\widetilde{\bar{\tilde{u}}_i}\,\widetilde{\bar{\tilde{u}}_j}. \tag{28}$$

This model is based on the scale-similarity assumption between $B_{ij}=\overline{\bar{u}_i\bar{u}_j}-\bar{u}_i\bar{u}_j$ and τ_{ij}. The link also appears in Ref. 4 and in an appendix of Ref. 32 which provides a few terms of the exact expansion for B_{ij}. The complete series can also be obtained, see Ref. 6. Using Eq. (5), it is easily verified that the first term in the expansion of B_{ij} is indeed the tensor-diffusivity model:

$$\begin{aligned}B_{ij}&=\left(\bar{\tilde{u}}_i\bar{\tilde{u}}_j+\frac{\overline{\Delta}^2}{2}\partial_k\partial_k(\bar{\tilde{u}}_i\bar{\tilde{u}}_j)+\cdots\right)-\left(\bar{\tilde{u}}_i+\frac{\overline{\Delta}^2}{2}\partial_k\partial_k\bar{\tilde{u}}_i+\cdots\right)\\&\quad\times\left(\bar{\tilde{u}}_j+\frac{\overline{\Delta}^2}{2}\partial_k\partial_k\bar{\tilde{u}}_j+\cdots\right)\\&=\frac{\overline{\Delta}^2}{2}(\partial_k\partial_k(\bar{\tilde{u}}_i\bar{\tilde{u}}_j)-(\bar{\tilde{u}}_i\partial_k\partial_k\bar{\tilde{u}}_j+\bar{\tilde{u}}_j\partial_k\partial_k\bar{\tilde{u}}_i))+\cdots\\&=\overline{\Delta}^2\partial_k\bar{\tilde{u}}_i\partial_k\bar{\tilde{u}}_j+\cdots.\end{aligned} \tag{29}$$

The other terms are, however, different from those in the exact reconstruction series. The scale-similarity model is thus not identical to the tensor-diffusivity model. In fact, *a priori* tests systematically indicate that the tensor-diffusivity model corresponds to better reconstruction of the filtered-scale stress. Nevertheless, since Bardina's model also corresponds to significant reconstruction,[13,24] the combination ''scale-similarity model supplemented by a Smagorinsky term'' also appears as a practical model for LES with explicit filtering.

Finally, one can also consider a ''clipped'' tensor-diffusivity model, with a limiter on the directional backscatter. One then removes the Smagorinsky term and adds a C coefficient in front of the clipped model. In a way, the method developed and tested in Refs. 33 and 34 (and based on developments in vortex methods[35]) is the integral formulation of this clipping approach. The main advantage of the integral formulation is that it provides for an easy way of identifying and clipping the direction(s) with backscatter. The clipping approach corresponds to a nonisotropic modification of the tensor-diffusivity model, and appears as a promising nonisotropic model. The mixed model used here is isotropic: The tensor-diffusivity reconstruction part and the dynamic Smagorinsky modeling part are both isotropic.

VI. THE DYNAMIC PROCEDURE APPLIED TO THE MIXED MODEL

As mentioned previously, the model coefficient, C, is obtained through the dynamic procedure,[16–20] here extended to the mixed model (22). It is obtained as follows.

(1) One applies an additional explicit test filter, $\hat{G}$, which is such that the combined $\widehat{\bar{G}}$ filtering is similar to the original $\bar{G}$ filtering.
(2) Recalling that the exact effective stress is $\tilde{\mathcal{T}}_{ij}$ with $\mathcal{T}_{ij}=\overline{u_iu_j}-\bar{\tilde{u}}_i\bar{\tilde{u}}_j$, it follows that the exact effective stress at the coarser test level is $\tilde{T}_{ij}^{c}$ with $T_{ij}=\widehat{\overline{u_iu_j}}-\widehat{\bar{\tilde{u}}_i^{c}}\,\widehat{\bar{\tilde{u}}_j^{c}}$ (here $\tilde{f}^{c}$ means $\tilde{f}$ further truncated to the coarser test grid). Thus, Germano's identity is here obtained as $T_{ij}-\widehat{\mathcal{T}_{ij}}=\widehat{\bar{\tilde{u}}_i\bar{\tilde{u}}_j}-\widehat{\bar{\tilde{u}}_i^{c}}\,\widehat{\bar{\tilde{u}}_j^{c}}\overset{\text{def}}{=}L_{ij}$, and thus, for the effective part, $\tilde{T}_{ij}^{c}-\widehat{\tilde{\mathcal{T}}_{ij}^{c}}=\tilde{L}_{ij}^{c}$.
(3) One uses effective stress models that are similar at both levels: $\tilde{\mathcal{T}}_{ij}^{M}$ taken similar to $\tilde{T}_{ij}^{c\,M}$, and with the same C.
(4) Using the similar models, one satisfies Germano's identity in the least-square sense: Defining the effective error tensor $\tilde{E}_{ij}^{c}=\tilde{L}_{ij}^{c}-(\tilde{T}_{ij}^{c\,M}-\widehat{\tilde{\mathcal{T}}_{ij}^{c\,M}})$, one minimizes $\langle\tilde{E}_{ij}^{c}\,\tilde{E}_{ij}^{c}\rangle$, where the integration $\langle\cdots\rangle$ is done over the homogeneous flow direction(s).

C is thus uniform along the homogeneous direction(s). Along the nonhomogeneous direction(s), if any, it is here also assumed that the spatial variation of C with respect to the test filter can be factored out, i.e., that $C\,\widehat{\tilde{a}_{ij}^{c}}\simeq C\,\widehat{\tilde{a}_{ij}^{c}}$.

If the explicit filter is Gaussian, $\bar{\mathcal{G}}(k)=\exp(-k^2\overline{\Delta}^2/2)$, the combined filter must also be Gaussian: $\widehat{\bar{\mathcal{G}}}(k)=\exp(-\alpha^2k^2\overline{\Delta}^2/2)$, i.e., $\widehat{\overline{\Delta}}/\overline{\Delta}=\alpha$. The explicit part of the test filter is also Gaussian:

$$\hat{\mathcal{G}}(k)=\widehat{\bar{\mathcal{G}}}(k)/\bar{\mathcal{G}}(k)=\exp(-(\alpha^2-1)\,k^2\overline{\Delta}^2/2). \tag{30}$$

Typically, we use $\alpha=2$. This test filter can only be applied in Fourier space: It is used only with spectral methods.

A useful explicit filter for working in physical space (e.g., using finite differences) is the top hat filter with $\overline{\Delta}_c$ taken as twice the LES grid size: $\bar{\mathcal{G}}(k)=\sin(k\Delta)/(k\Delta)$, and thus $\widehat{\bar{\mathcal{G}}}(k)=\sin(\alpha k\Delta)/(\alpha k\Delta)$. If we use $\alpha=2$, the required test filter is obtained as[36]

$$\hat{\mathcal{G}}(k)=\widehat{\bar{\mathcal{G}}}(k)/\bar{\mathcal{G}}(k)=\sin(2\,k\Delta)/(2\sin(k\Delta))=\cos(k\Delta), \tag{31}$$

which, in physical space, is simply the *discrete arithmetic mean* filter:

$$\hat{G}(x)=(\delta(x+\Delta)+\delta(x-\Delta))/2. \tag{32}$$

This test filter is conveniently applied in physical space, using only the near neighbor grid values, see Sec. VIII. (It can also be applied in Fourier space.)

The dynamic procedure for the mixed model is here summarized:

Downloaded 10 May 2001 to 128.206.16.97. Redistribution subject to AIP license or copyright, see http://ojps.aip.org/phf/phfcr.jsp

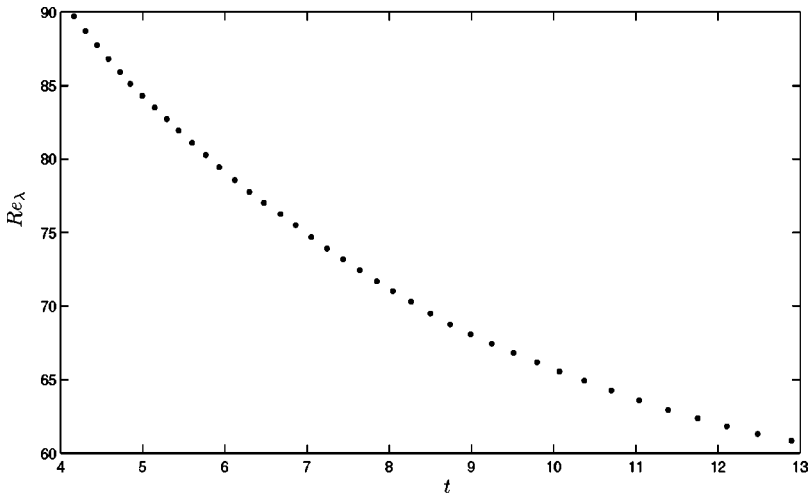

FIG. 1. Evolution of Re_λ for the reference DNS.

$$m_{ij}=\overline{\Delta}_k^2\,\partial_k\tilde{\bar{u}}_i\,\partial_k\tilde{\bar{u}}_j,\quad a_{ij}=2\,\Delta^2\,|\tilde{\bar{S}}|\,\tilde{\bar{S}}_{ij},\quad \widetilde{\mathcal{T}}_{ij}^{M}=\tilde{m}_{ij}-C\,\tilde{a}_{ij},$$

$$M_{ij}=\alpha^2\,\overline{\Delta}_k^2\,\partial_k\widehat{\tilde{\bar{u}}_i^c}\,\partial_k\widehat{\tilde{\bar{u}}_i^c},\quad A_{ij}=2\,\alpha^2\,\Delta^2\,|\widehat{\tilde{\bar{S}}^c}|\,\widehat{\tilde{\bar{S}}_{ij}^c},\tag{33}$$

$$\tilde{T}_{ij}^{c\,M}=\tilde{M}_{ij}^c-C\,\tilde{A}_{ij}^c,\quad \tilde{p}_{ij}^c=\tilde{L}_{ij}^c+(\widehat{\tilde{m}_{ij}^c}-\tilde{M}_{ij}^c),\quad \tilde{q}_{ij}^c=\widehat{\tilde{a}_{ij}^c}-\tilde{A}_{ij}^c,$$

$$C=\frac{\langle\tilde{p}_{ij}^c\,\tilde{q}_{ij}^c\rangle}{\langle\tilde{q}_{kl}^c\,\tilde{q}_{kl}^c\rangle}=\frac{\langle\tilde{p}_{ij}^{c\,*}\,\tilde{q}_{ij}^{c\,*}\rangle}{\langle\tilde{q}_{kl}^{c\,*}\,\tilde{q}_{kl}^{c\,*}\rangle}.$$

For homogeneous decaying turbulence, one obtains $C=C(t)$. For the channel flow, two directions are homogeneous so that $C=C(y,t)$. Since the channel flow dynamical LES eventually reaches statistical equilibrium, time averaging can also be done and one ends up with $C(y)$.

VII. RESULTS FOR LES OF ISOTROPIC TURBULENT DECAY

The results presented here were obtained using the mixed model and with explicit Gaussian filtering: $\overline{\mathcal{G}}(k)=\exp(-k^2\,\overline{\Delta}^2/2)$. Other filters could have been used. The solver is a pseudospectral code with shift dealiasing done on all products. The modes are truncated in wave space, using spherical truncation. The reference data are a 256^3 DNS that was run using the same code. It was started using a field with given spectra and random phases. This initial condition then evolved into real turbulence. The reference DNS data cover a usable window of Re_λ from 90 to 60, see Fig. 1. At the begining of the window ($t=4.17$, $\mathrm{Re}_\lambda\approx 90$), the Kolmogorov scale, $\eta=(\nu^3/\langle\epsilon\rangle)^{1/4}$, is such that $k_{\max}\,\eta\approx 2$: typical of a well-resolved DNS. The $t=4.17$ DNS was truncated to 64^3 and was Gaussian filtered using $\overline{\mathcal{G}}(k)=\exp(-k^2\Delta^2/4)$ where $\Delta=(256/64)\,\Delta_{\mathrm{DNS}}$ is the LES grid size, see Fig. 2. Thus, we have $\overline{\Delta}_c=\sqrt{12}\,\overline{\Delta}=\sqrt{6}\,\Delta$. At the LES cutoff, this gives $\overline{\mathcal{G}}(\pi/\Delta)=\exp(-\pi^2/4)=0.085$: The amount of explicit filtering is thus significant. As to the dissipation spectrum of the DNS, see Fig. 11, it is still quite high at the LES cutoff (2.1×10^{-3}) and is close to the value for the ''inertial range'' (2.4×10^{-3} in the range $k\approx[19-25]$). For additional comparisons, two more challenging 48^3 LESs are also run, thus with cutoff right into the inertial range. Finally, in all cases where the dynamic procedure is applied, this is done using the usual value: $\alpha=\hat{\overline{\Delta}}/\overline{\Delta}=2$.

A. The tensor-diffusivity model alone

As a first *a priori* test of the tensor-diffusivity model, its correlation with the exact filtered-scale stress, τ_{ij}, was

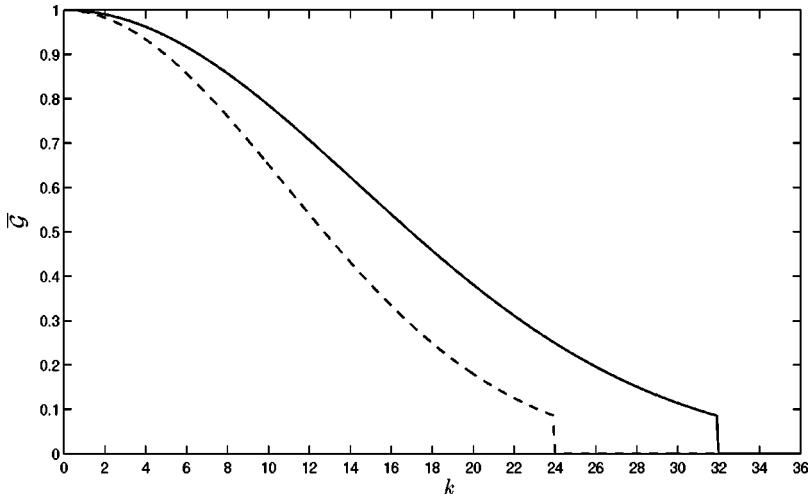

FIG. 2. The truncated Gaussian filters used for the 64^3 LES and the 48^3 LES with explicit filtering.

Downloaded 10 May 2001 to 128.206.16.97. Redistribution subject to AIP license or copyright, see http://ojps.aip.org/phf/phfcr.jsp

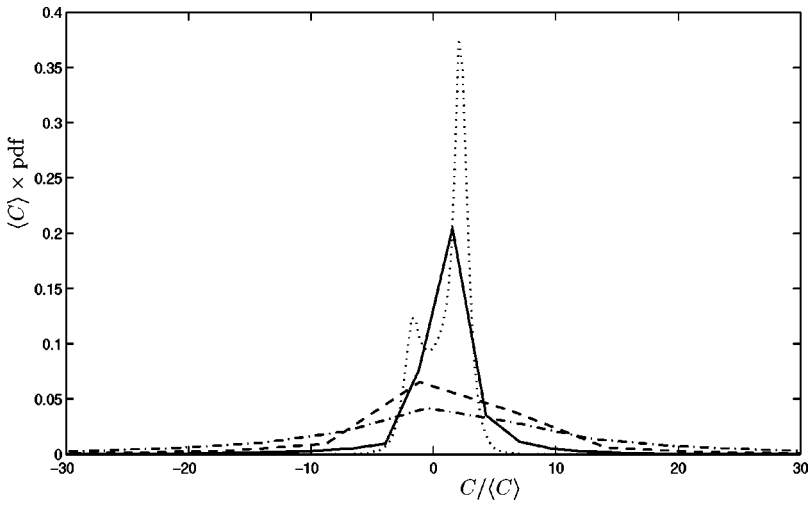

FIG. 3. Normalized pdf for the dynamic coefficient at $t=4.17$ (dynamic procedure done locally): dynamic tensor diffusivity model (dotted line); dynamic Smagorinsky term in the mixed model (solid line); dynamic Smagorinsky model (dashed line); dynamic Smagorinsky model without explicit filtering (chained-dotted line).

evaluated, using the complete DNS (no truncation) filtered using $\overline{\mathcal{G}}(k)=\exp(-k^2\Delta^2/4)$ with $\Delta=(256/64)\,\Delta_{\mathrm{DNS}}$:

$$\eta_1=\frac{\langle \tau_{ij}^M\,\tau_{ij}\rangle}{\langle \tau_{ij}\,\tau_{ij}\rangle^{1/2}\langle \tau_{ij}^M\,\tau_{ij}^M\rangle^{1/2}}=\frac{15.47}{5.21\times 3.21}=0.925,$$
$$\eta_2=\frac{\langle \tau_{ij}^M\,\tau_{ij}\rangle}{\langle \tau_{ij}\,\tau_{ij}\rangle}=0.570. \tag{34}$$

The η_1 correlation is thus quite high, confirming that this model is well aligned with the exact filtered-scale stress. The variances are however different, 3.21 compared to 5.21 (the ratios being 3.21/5.21=0.62 or, conversely, 1.62). Hence η_2 is significantly lower than η_1. Thus, the series truncated to the first term reconstructs a significant fraction of the filtered-scale stress but not all of it. Filtering using instead $\Delta=(256/48)\,\Delta_{\mathrm{DNS}}$ leads to $\eta_1=0.906$ (with variances of 3.46 and 6.17) and to $\eta_2=0.508$.

As a second *a priori* test, the dynamic procedure for LES truncated to 64^3 was applied to a dynamic version of the tensor-diffusivity model, $C\,\overline{\Delta}^2\partial_k\widetilde{\bar{u}_i\partial_k\bar{u}_j}$, using the truncated Gaussian filter, see Fig. 2. We obtained $C=1.17$ (higher than unity, yet not as high as 1.6). The dynamic procedure was able to determine a C level in the correct range. Recall that the procedure is not perfect: It is based on the modeled stresses, on the similarity assumption for the models over the relevant range (from the original LES scale to the coarser test scale), and on the scale similarity assumption of the LES fields over that range (something neither clear nor established).

Theoretically, once the explicit filter width is normalized, the coefficient in front of the tensor-diffusivity model is unity. But there are other terms in the reconstruction series. In view of the good alignment of the tensor-diffusivity model with the complete filtered-scale stress, it appears that modeling of the series truncation effects could be achieved by allowing a C in front of the tensor-diffusivity model. Alone, this model does not work for long times in LES runs. Adding the necessary modeling for the subgrid-scale effects, here using a Smagorinsky term, would then lead to a mixed model with two coefficients to determine. Here, we chose instead to retain and investigate the mixed model as in Eq. (22), the only coefficient being that in front of the dynamic Smagorinsky term: Modeling of all truncation effects (truncation of the reconstruction series and subgrid-scale stress) is thus lumped into the dynamic Smagorinsky term.

As another a priori test, the dynamic procedure for 64^3 LES was again applied to the tensor-diffusivity model, but locally (i.e., no averaging over the homogeneous directions): C is then a function of space. The pdf (probability density function) of C is also obtained, with $\int \mathrm{pdf}(C)\,dC=1$ and $\langle C\rangle=\int C\,\mathrm{pdf}(C)\,dC=0.63$. Here, the dynamic coefficient is, on average, less than unity. The normalized pdf is shown in Fig. 3: We notice that it is not symmetric but bimodal. The positive mode is, however, quite sharp (as expected, since the model acts as good partial reconstruction of the filtered-scale stress), and of significantly higher amplitude than the negative mode. For comparison, we also provide the normalized pdf when the dynamic Smagorinsky model is used alone (i.e., no filtered-scale stress reconstruction). The pdf (with $\langle C\rangle=0.041$) is almost symmetric: almost as many negative C values as positive ones, confirming that this model alone is a poor model for the total effective stress (filtered-scale stress+subgrid-scale stress).

We now examine the results of LES runs done using the tensor-diffusivity model alone. For this section and the following, the LES runs are 64^3, with shift dealiasing and spherical truncation of radius $k_{\max}=31$. (In later additional comparisons, two 48^3 LES runs are also done.) Moreover, the quantities such as resolved energy spectra, $E_r(k)$, resolved energy, $\langle E_r\rangle=\int_0^{k_{\max}}E_r(k)\,dk$, and resolved enstrophy, $\langle \mathcal{E}_r\rangle=\int_0^{k_{\max}}k^2\,E_r(k)\,dk$, are all evaluated by defiltering the LES results, i.e., by using $E_r(k)=\exp(k^2\overline{\Delta}^2)\,E(k)$ where $E(k)$ is the spectrum of the filtered and truncated field. This allows for straightforward and severe comparison with the truncated DNS results.

Since the initial condition has negative skewness, the tensor-diffusivity model should, in principle, lead to a simulation that does not blow up globally, even if the global dissipation is found to be too low. The problem is the numerics: Is such a simulation feasible? One could argue that the model is numerically ill-conditioned as it corresponds to

Downloaded 10 May 2001 to 128.206.16.97. Redistribution subject to AIP license or copyright, see http://ojps.aip.org/phf/phfcr.jsp

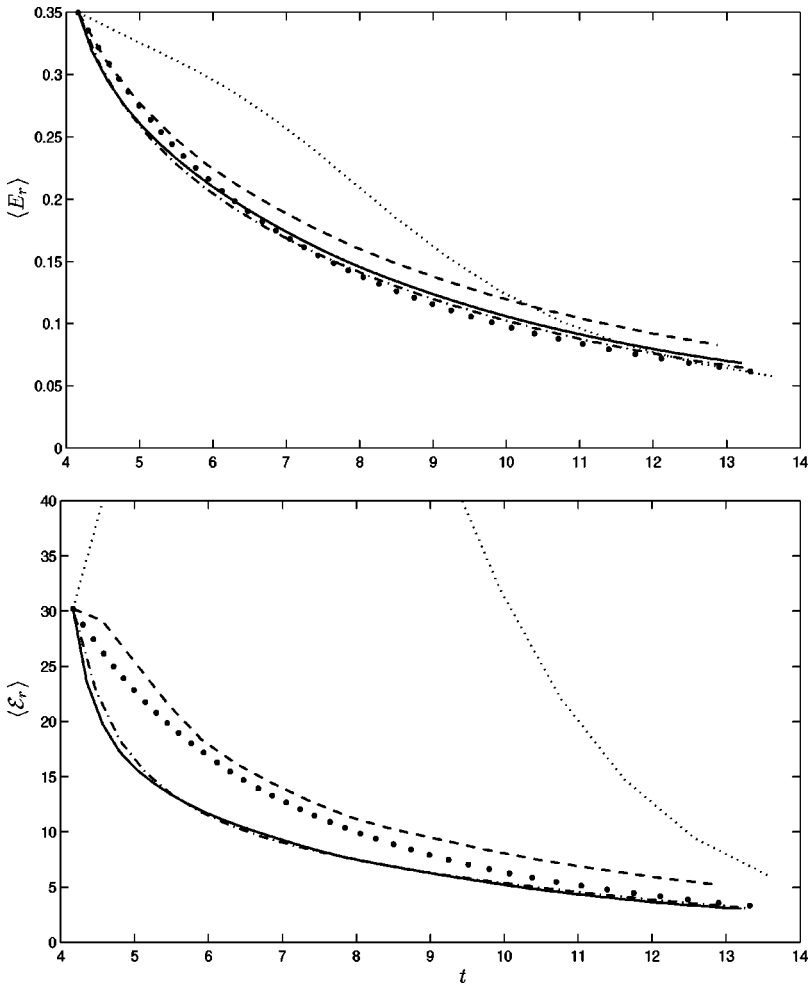

FIG. 4. Evolution of the energy and enstrophy associated with the 64^3 resolved field: truncated DNS (closed circle); tensor-diffusivity model (dotted line); dynamic mixed model (tensor diffusivity+dynamic Smagorinsky) (solid line); dynamic Smagorinsky model (dashed line); dynamic Smagorinsky model without explicit filtering (chained-dotted line).

negative diffusion along the local direction(s) of stretching, and thus that it must lead to numerical blow up. Our numerical experiments show that this is not the case: The simulation remains stable (as long as the skewness of the LES fields remains negative). This is a remarkable, nontrivial result. This success is due to the fact that the direction(s) of negative diffusion continuously evolve in space and time. The negative diffusion continuously changes direction(s) and is counterbalanced by positive diffusion, the whole simulation remaining globally stable and dissipative. Thus, a pure tensor-diffusivity simulation is feasible. In analogous studies of turbulent flow in a mixing layer,[4,5] the tensor-diffusivity model, in combination with a central fourth-order accurate discretization, was shown to result in stable simulations as well. The tensor-diffusivity model plays its role: provides for significant, yet partial, reconstruction of the filtered-scale stress, $\tilde{\mathcal{B}}_{ij}$, and thus for local backscatter, while remaining globally dissipative (as long as the skewness of the LES fields remains negative).

However, as expected from the above-mentioned *a priori* tests, the tensor-diffusivity model alone provides too little global dissipation for the filtered and truncated field, $\bar{\tilde{u}}_i$, even at the start, see Figs. 4 and 5. Initially, the tensor-diffusivity dissipation is 4.1×10^{-2}, which is substantially lower than that due to the exact effective stress (filtered scale+subgrid scale): 6.8×10^{-2}. This was to be expected, as there is no truncation modeling so far. Roughly $4.1/6.8 = 60\%$ of the required model dissipation is nevertheless provided by the tensor-diffusivity model. Notice that this is close to the ratio for the measured variances (62%).

The energy and enstrophy curves are shown in Fig. 4: not enough energy decay and even an increase in the enstrophy. The dissipation of the filtered and truncated field is provided in Fig. 5. As to the evolution of the resolved energy spectra, they are given in Fig. 8: The tensor-diffusivity model alone is not active enough at high wave numbers; an added truncation model is required in order to prevent the lifting up, as the LES evolves, of the energy spectra after $k \approx 10$.

B. The mixed model

As an interesting *a priori* test of the mixed model, Eq. (22), the dynamic procedure was also applied locally. The normalized pdf of the dynamic C in the Smagorinsky term (with $\langle C \rangle = 0.11$) is shown in Fig. 3. Since the tensor-diffusivity model has properly reconstructed a significant fraction of the filtered-scale stress, the remaining part is, as usual, hard to model by a Smagorinky term, hence a wide, almost symmetric, pdf.

It is instructive to compare this pdf with that obtained when examining the dynamic Smagorinsky model for LES

Downloaded 10 May 2001 to 128.206.16.97. Redistribution subject to AIP license or copyright, see http://ojps.aip.org/phf/phfcr.jsp

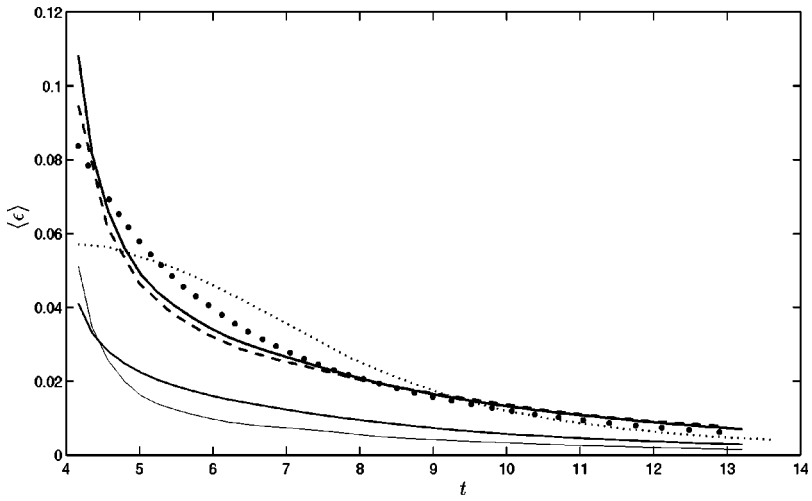

FIG. 5. Evolution of the dissipation associated with the 64^3 resolved and filtered field: truncated and filtered DNS (closed circle); tensor-diffusivity model (dotted line); dynamic mixed model (solid line): tensor-diffusivity term (thin solid line), and dynamic Smagorinsky term (thinner solid line); dynamic Smagorinsky model (dashed line).

without explicit filtering (i.e., pure truncation, here with sharp Fourier cutoff, and a dynamic procedure using the sharp Fourier cutoff as test filter, with $\langle C\rangle = 0.016$), see Fig. 3. The normalized pdf of the Smagorinsky coefficient in the mixed model is seen to be significantly better than the normalized pdf of the Smagorinsky coefficient for LES without explicit filtering: It is sharper and thus more skewed to positive C values. This supports the thesis, also developed in Ref. 6, that the use of explicit filtering in LES might allow for easier modeling of the truncation effects. In particular, the dynamic Smagorinsky term might be a better truncation model in LES with explicit filtering (and thus with mixed modeling) than in LES without explicit filtering. The hope is thus to also obtain better results in actual LES runs. We will see in the following that this is not the case: The results are about the same. Once again, one finds that *a priori* tests are only part of the story in LES.

We now examine the results obtained when running the dynamic mixed model: tensor-diffusivity model+dynamic Smagorinsky term. It is seen, in Fig. 4, that the dynamic mixed model also does not start with the correct energy decay slope. It is also observed, in Fig. 5, that the initial dissipation of the filtered and truncated field, $\bar{\tilde{u}}_i$, is too large: The model dissipation is $(4.1+5.1)\times 10^{-2}$ (4.1 for the tensor-diffusivity contribution and 5.1 for the dynamic Smagorinsky contribution), and the viscous dissipation is 1.6×10^{-2}, leading to a total of 10.8×10^{-2}. This is to be compared with 8.4×10^{-2} for the filtered and truncated DNS. The reason for this initial ''anomaly'' is that the dynamic procedure initially has a hard time finding the proper C value: The initial value, $C=6.3\times 10^{-2}$, is too large; hence the dynamic Smagorinsky term dissipates too much initially; in particular, it initially dissipates more than the tensor-diffusivity term. However, C is seen to decrease rapidly, see Fig. 6, with stabilization at $C\approx 3.2\times 10^{-2}$. It then continues to decrease slowly as the LES proceeds. When the dynamic procedure has stabilized, it is seen that the dynamic Smagorinsky term dissipates less than the tensor-diffusivity term, see Fig. 5, and that the ratio between the two terms contributions then remains fairly constant in time (at about 0.5–0.6) indicating a good self-similar behavior of the mixed model, as one would expect.

We conclude that the dynamic procedure clearly needs to ''settle in.'' The poor initial performance on decay is to be attributed to the initial transients of the dynamic procedure, not to the mixed model. This initial transient is observed with all LES models. It relates to the fact that the LES field needs to evolve from what it ''receives as initial condition'' (here, the best possible one since it corresponds to a DNS

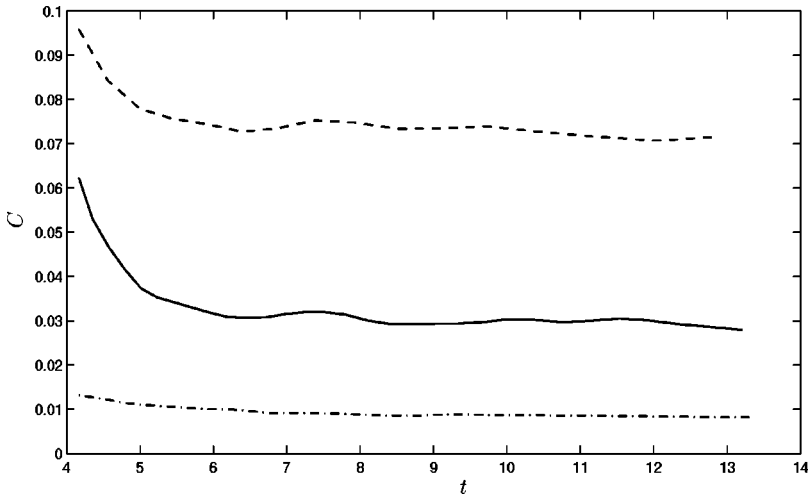

FIG. 6. Evolution of the dynamic coefficient (dynamic procedure done globally): dynamic Smagorinsky term in mixed model (solid line); dynamic Smagorinsky model (dashed line); dynamic Smagorinsky model without explicit filtering (chained-dotted line).

Downloaded 10 May 2001 to 128.206.16.97. Redistribution subject to AIP license or copyright, see http://ojps.aip.org/phf/phfcr.jsp

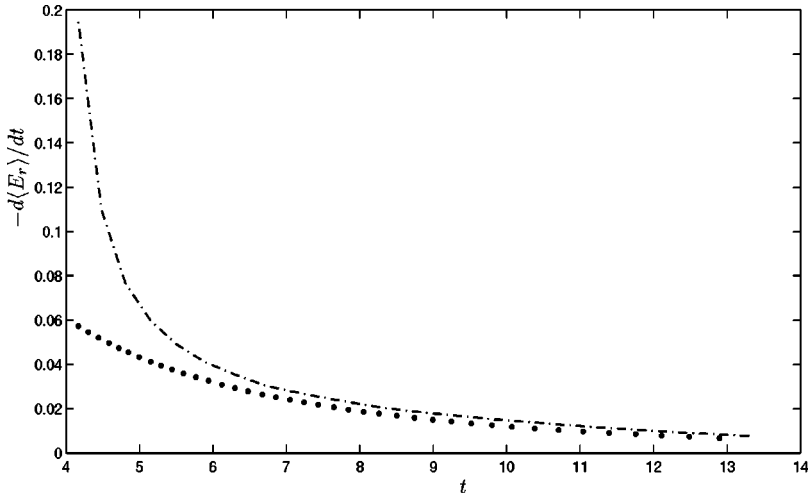

FIG. 7. Evolution of the dissipation associated with the 64^3 resolved field: truncated DNS (closed circle); dynamic Smagorinsky model without explicit filtering (chained-dotted line).

that was explicitly filtered and truncated) to what corresponds to ''its own statistical equilibrium'' (an equilibrium with a spectrum compatible with the LES grid and model used). This ''self-restoring'' property which is inherent in the dynamic approach has also been observed in relation to other flows.[37] Had the dynamic procedure produced $C \approx 3.2 \times 10^{-2}$ from the start, the dissipation would have been correct initially: A Smagorinsky contribution of approximately $(3.2/6.2) \times 5.1 \times 10^{-2} = 2.6 \times 10^{-2}$, leading to a total dissipation of 8.3×10^{-2}: very close to the exact value of 8.4×10^{-2}.

For comparison, we consider next the dynamic Smagorinsky model alone, with same explicit filtering: thus, no partial reconstruction of the filtered-scale stress. It starts off with the correct energy decay slope, see Fig. 4, but it then underdissipates, see Fig. 5. Here, the dynamic C is correct initially (i.e., the obtained $C = 9.6 \times 10^{-2}$, see Fig. 6, produces the proper initial dissipation for the model, see Fig. 5), but, since C also decreases during the initial transient to stabilize at $C \approx 7.5 \times 10^{-2}$, the model underdissipates at later times.

The dynamic Smagorinsky model for classical LES without explicit filtering is also run for reference comparison: Eq. (13) with $\tilde{\mathcal{A}}_{ij}^M = -2\, C\, \Delta^2\, \widetilde{|\tilde{S}|\, \tilde{S}}_{ij}$ and dynamic C with sharp Fourier cutoff used as test filter. The obtained energy decay for the resolved field is found to be almost identical to what is obtained when using the mixed model with explicit filtering, see Fig. 4. This is also true for all other diagnostics, see the following. These results are most interesting: They confirm that the dynamic mixed model for LES with explicit filtering is capable of the same performance as the dynamic Smagorinsky model for LES without explicit filtering. These results also support the thesis that the necessary partial reconstruction term (here tensor diffusivity) might also be sufficient in practice. They are, however, disappointing with respect to expectations built on favorable *a priori* tests of the mixed model (see Sec. VII A and Ref. 6).

The dissipation rate for the resolved field is provided in Fig. 7. It is also too large initially, but it quickly comes down to the correct level. Thus, the dynamic Smagorinsky model for LES without explicit filtering (and here with shift dealiasing) is not exempt of the initial anomaly, even when started from a truncated DNS.

Comparisons are also made on the decay of global enstrophy (which puts more emphasis on the high end of the spectrum), see Fig. 4. Again, the results for the dynamic mixed model and for the dynamic Smagorinsky model without explicit filtering are very close, with initially too much decay of enstrophy.

The energy spectra can also be compared: The reconstructed spectra, $E_r(k)$, at $t \approx 4.5$, $t \approx 7.5$, and $t \approx 9.0$ are shown in Fig. 8. Again, the results for the dynamic mixed model and for the dynamic Smagorinsky model without explicit filtering are very close: almost identical spectra over the whole range of wave numbers. The usual shortcomings of the Smagorinsky model are present in both cases: its inability to properly differentiate between large and small scales. Finally, the spectra obtained when using the dynamic Smagorinsky model alone, and with explicit filtering, are clearly not as good: This confirms that partial reconstruction of the filtered-scale stress is required.

A final remark: We here used shift dealiasing for all products (including those in the dynamic procedure), and spherical truncation of the modes in wave space. Using 3/2 dealiasing instead leads to a different (and better) initial C for the dynamic Smagorinsky model, hence to a different (and better) initial decay of the resolved energy.[29] The difference is to be found in the fact that one then uses more information to evaluate the dynamic C.

C. Spectrum of dissipation

For the mixed model a central question, which we address here, concerns which part of the model does what in terms of dissipation. We here investigate the contribution of the different terms to the *spectrum of dissipation* for the filtered and truncated field. In Fourier space, we denote the conjugate of any function g by g^c. Then, for each effective $\tilde{q}_{ij}$ term (viscous, model, or convection term), it is easily shown, since $\tilde{q}_{ij} = \tilde{q}_{ji}$, that its contribution to the spectrum of dissipation is

Downloaded 10 May 2001 to 128.206.16.97. Redistribution subject to AIP license or copyright, see http://ojps.aip.org/phf/phfcr.jsp

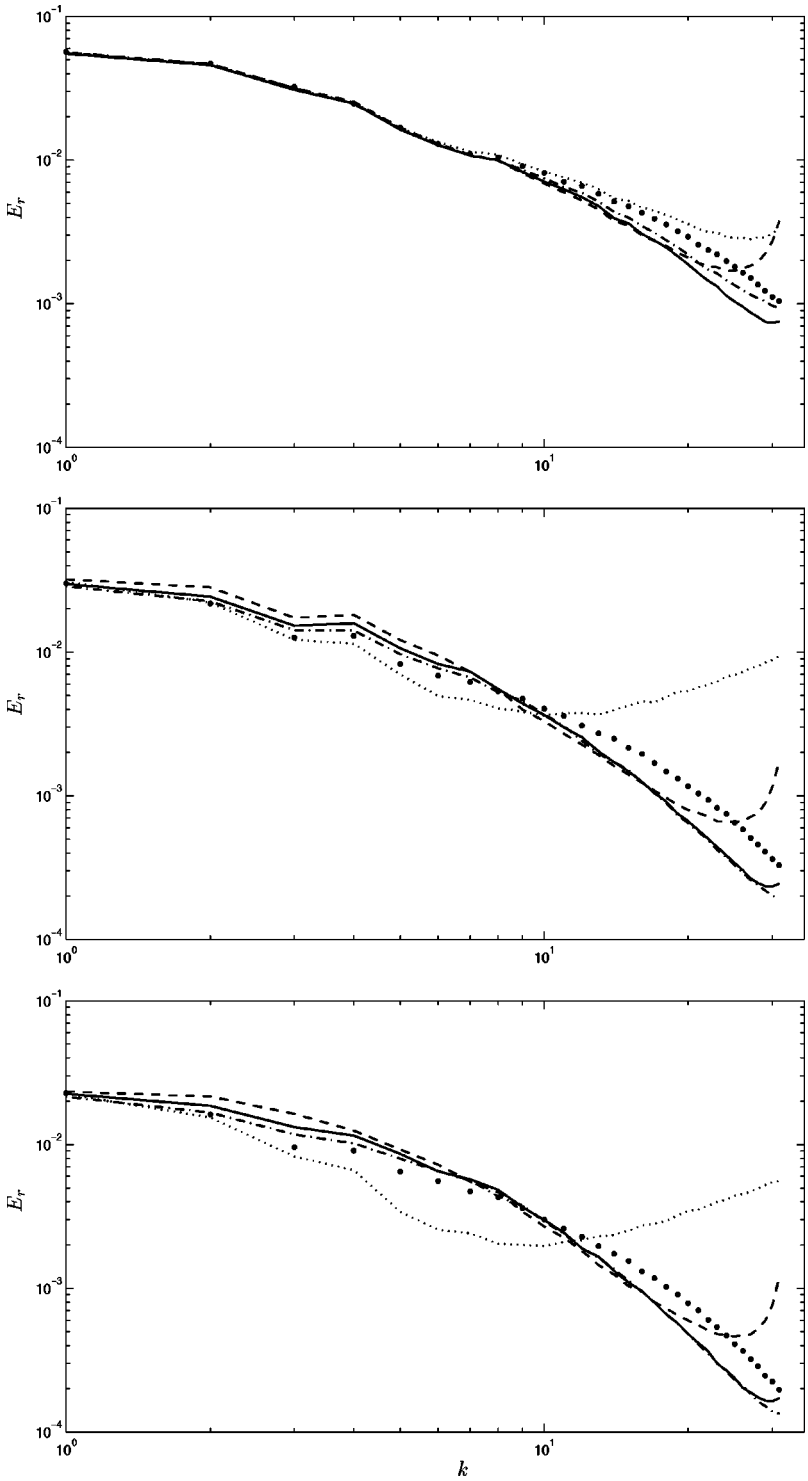

FIG. 8. Spectrum of the 64^3 resolved energy at $t \approx 4.5$, $t \approx 7.5$ and $t \approx 9.0$: truncated DNS (closed circle); tensor diffusivity model (dotted line); dynamic mixed model (tensor-diffusivity+dynamic Smagorinsky) (solid line); dynamic Smagorinsky model (dashed line); dynamic Smagorinsky model without explicit filtering (chained-dotted line).

$$\epsilon_q(\mathbf{k}) = -\frac{1}{2}\frac{d}{dt}(\bar{\tilde{u}}_i(\mathbf{k})\,\bar{\tilde{u}}_i^c(\mathbf{k}))$$

$$= -\frac{1}{2}\left(\frac{d\bar{\tilde{u}}_i}{dt}(\mathbf{k})\bar{\tilde{u}}_i^c(\mathbf{k}) + \frac{d\bar{\tilde{u}}_i^c}{dt}(\mathbf{k})\bar{\tilde{u}}_i(\mathbf{k})\right)$$

$$= \frac{1}{2}(ik_j\tilde{q}_{ij}(\mathbf{k})\bar{\tilde{u}}_i^c(\mathbf{k}) - ik_j\tilde{q}_{ij}^c(\mathbf{k})\bar{\tilde{u}}_i(\mathbf{k}))$$

$$= \frac{1}{2}(ik_j\,\bar{\tilde{u}}_i^c(\mathbf{k})\tilde{q}_{ij}(\mathbf{k}) - ik_j\,\bar{\tilde{u}}_i(\mathbf{k})\tilde{q}_{ij}^c(\mathbf{k}))$$

$$= -\frac{1}{2}(\bar{\tilde{S}}_{ij}^c(\mathbf{k})\tilde{q}_{ij}(\mathbf{k}) + \bar{\tilde{S}}_{ij}(\mathbf{k})\tilde{q}_{ij}^c(\mathbf{k})), \tag{35}$$

which is indeed a real function of $\mathbf{k}$. The k-shell contribution of this function is what we call the spectrum of dissipation associated with the q_{ij} term; it is its contribution to the time derivative of the energy in that shell:

$$\frac{d}{dt}E(k) = -\epsilon(k) = -\sum_q \epsilon_q(k). \tag{36}$$

Downloaded 10 May 2001 to 128.206.16.97. Redistribution subject to AIP license or copyright, see http://ojps.aip.org/phf/phfcr.jsp

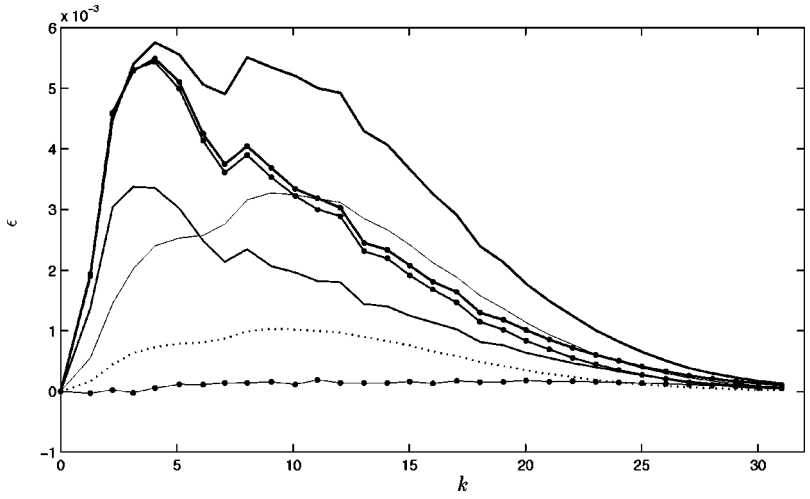

FIG. 9. Spectrum of dissipation for the 64^3 resolved and filtered field at $t=4.17$. Contributions of the different stresses: $\tilde{\mathcal{T}}_{ij}$ from the DNS (solid line+circle): $\tilde{\mathcal{B}}_{ij}$ (thin solid line+circle) and $\tilde{\bar{\mathcal{A}}}_{ij}$ (thinner solid line+circle); $\tilde{\mathcal{T}}_{ij}^{M}$ in the mixed model (solid line): tensor-diffusivity term (thin solid line) and dynamic Smagorinsky term (thinner solid line); viscous stress (dotted line).

One can thus examine the dissipation shell by shell and term by term. As to global quantities, they are obtained in physical space or in Fourier space since one can also write

$$\frac{d}{dt}\int_0^{k_{\max}} E(k)\,dk = \frac{d}{dt}\langle E\rangle = -\langle \epsilon\rangle = -\int_0^{k_{\max}} \epsilon(k)\,dk$$

$$= -\sum_q \int_0^{k_{\max}} \epsilon_q(k)\,dk. \tag{37}$$

Figure 9 provides the dissipation spectra associated with the modeled and exact stresses. This corresponds to the initial condition (hence the contribution of the dynamic Smagorinsky term is too high; it is lower at later times).

(1) Even though the exact $\tilde{\mathcal{B}}_{ij}$ stress (and its tensor-diffusivity model) have positive and negative values of local dissipation in physical space, we confirm that the dissipation spectrum is positive for all k shells relevant to the LES.

(2) The shape of the spectrum associated with the tensor-diffusivity model contribution is similar to that of the exact $\tilde{\mathcal{B}}_{ij}$, confirming again that this term acts as good partial reconstruction. Because the reconstruction is incomplete, the amplitude is too low. In the present mixed model, the difference between the integrals must also be captured by the truncation model: here the Smagorinsky term.

(3) It is interesting to consider the ratio of the exact effective stress contribution, $\tilde{\mathcal{T}}_{ij}$, divided by the tensor-diffusivity contribution, see Fig. 10: It is fairly constant, except at the high wave numbers, which indicates again that the subgrid-scale effects are important. It would be tempting to multiply the tensor-diffusivity model by a factor close to 1.6 (i.e., also close to the ratio of variances from the *a priori* tests) and run the LES without added subgrid-scale modeling. Even if this provides the correct dissipation initially, this does not work for long: Without subgrid-scale modeling, the simulation quickly leads to lifting up of the energy spectrum, much in the same way as what was obtained when running the tensor-diffusivity model alone with unit factor, see Fig. 8.

(4) The shape of the spectrum associated with the Smagorinsky term is similar to that associated with the viscous term, confirming that the nonuniformity in the $1/T$ scaling for the effective viscosity has little impact in homogeneous flows.

(5) The spectra of the two model terms are very different in shape, and their peak contributions are in clearly distinct zones. They are thus complementary.

For completeness, we also provide, in Fig. 11, the dissipation spectrum for the complete DNS field. We observe an

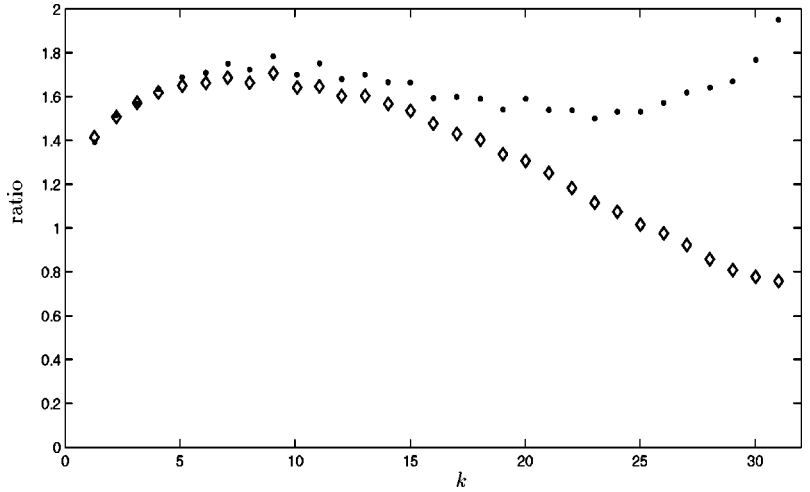

FIG. 10. Ratio between dissipation spectra: exact $\tilde{\mathcal{T}}_{ij}$ contribution divided by tensor-diffusivity contribution (circle); exact $\tilde{\mathcal{B}}_{ij}$ contribution divided by tensor-diffusivity contribution (diamond).

Downloaded 10 May 2001 to 128.206.16.97. Redistribution subject to AIP license or copyright, see http://ojps.aip.org/phf/phfcr.jsp

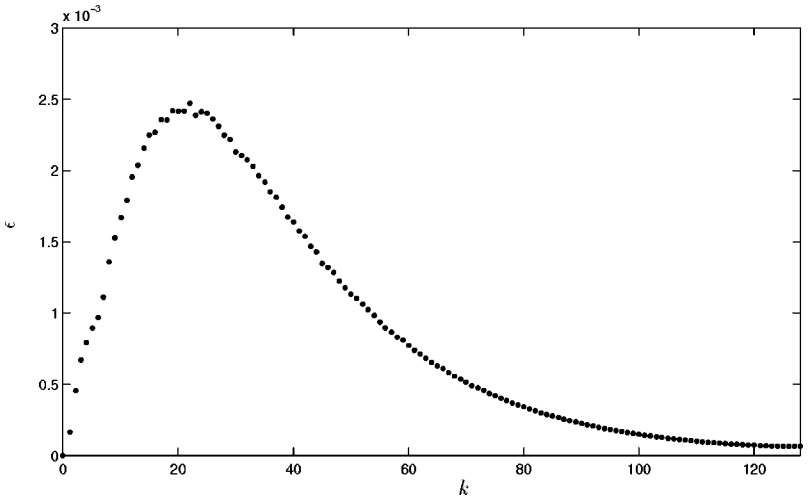

FIG. 11. Spectrum of dissipation for the viscous stress in the DNS.

inertial range with almost uniform dissipation for $k \approx [19-25]$, followed by a dissipation range. This figure helps realize why the LES model is needed: At the LES cutoff, the DNS still has significant dissipation (about 90% of that in the inertial range). One could not run without the LES model. For instance, in LES with explicit filtering, the model dissipation accounts for about 80% of the total required dissipation.

D. More challenging LES

As it can be argued that the previous 64^3 LES correspond to some overkill, smaller 48^3 LES (thus with cutoff well into the inertial range) were also run: dynamic mixed model with explicit filtering (using the truncated Gaussian filter, see Fig. 2), and dynamic Smagorinsky model without explicit filtering. The resolved energy and enstrophy results

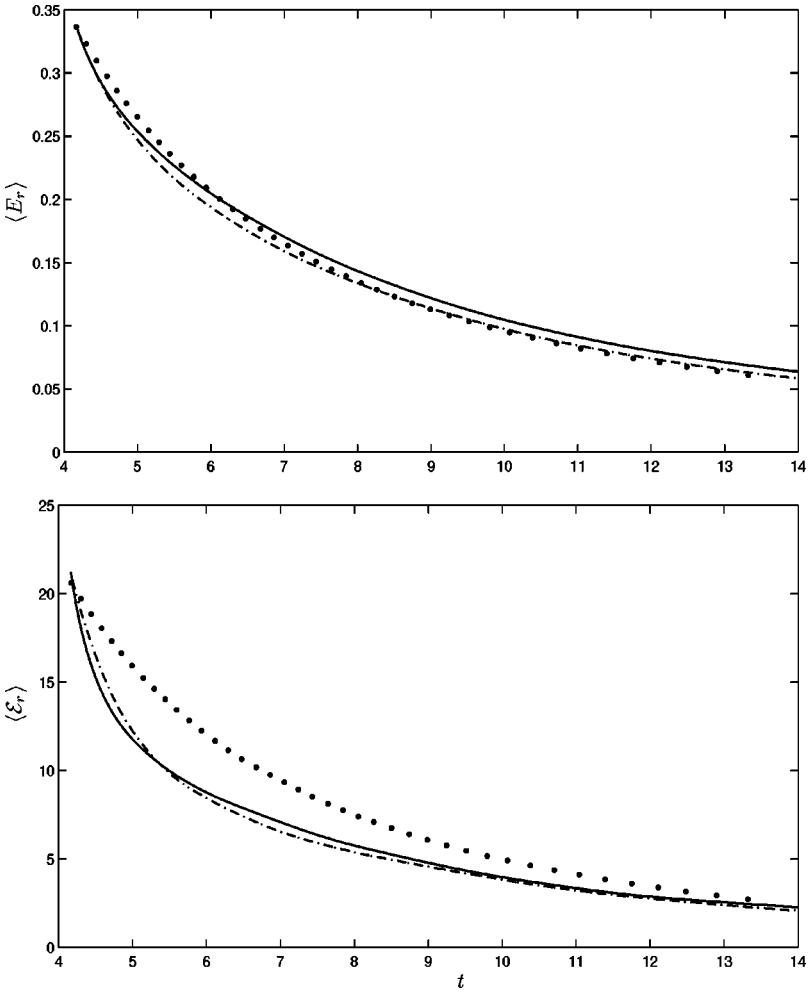

FIG. 12. Evolution of the energy and enstrophy associated with the 48^3 resolved field: truncated DNS (closed circle); dynamic mixed model (solid line); dynamic Smagorinsky model without explicit filtering (chained-dotted line).

Downloaded 10 May 2001 to 128.206.16.97. Redistribution subject to AIP license or copyright, see http://ojps.aip.org/phf/phfcr.jsp

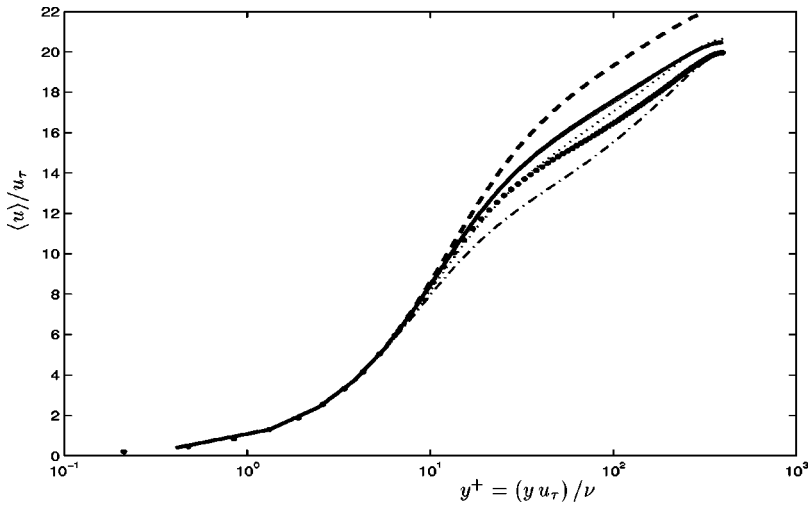

FIG. 13. Mean velocity profiles: DNS (closed circle), dynamic mixed model (tensor diffusivity+dynamic Smagorinsky), F1 (solid line) and F2 (thin solid line); dynamic Smagorinsky model, F1 (dash); dynamic Smagorinsky model without explicit filtering, $x-z$ sharp cutoff test filtering (dotted line), no model (chained-dotted line).

are shown in Fig. 12. Again, the results from both approaches do not differ significantly: The enstrophy curves are very much alike, and so are the energy curves for short times. Here, however, the energy curves differ at later times. Again, no conclusion can be drawn as to which model performs best. Their performances are comparable.

VIII. RESULTS FOR LES OF TURBULENT CHANNEL FLOW

Here, the solver is a fourth-order finite difference code.[38,39] The reference DNS is the one at $\mathrm{Re}_\tau = h\,u_\tau/\nu = 395$ of Refs. 40 and 41, where h is half the channel width and $u_\tau = \sqrt{\tau_w}$ is the friction velocity with τ_w the mean wall friction. The computational domain is $(L_x, L_y, L_z) = (2\pi, 2, \pi)h$. The DNS grid was $256\times193\times192$. We use a LES grid that cuts the DNS grid by a factor of 4 in each direction: $64\times49\times48$. The mixed model here becomes

$$\tilde{\mathcal{T}}_{ij}^{M} = \overline{\Delta}_x^2\, \partial_x \widetilde{\bar{u}_i}\, \partial_x \bar{u}_j + \overline{\Delta}_y^2\, \partial_y \widetilde{\bar{u}_i}\, \partial_y \bar{u}_j + \overline{\Delta}_z^2\, \partial_z \widetilde{\bar{u}_i}\, \partial_z \bar{u}_j - 2\, C\, \Delta^2\, \widetilde{|\bar{\bar{S}}|\, \bar{\bar{S}}_{ij}}, \tag{38}$$

where the effective Δ^2 for the dynamic Smagorinsky term is taken as $(\Delta_x\, \Delta_y\, \Delta_z)^{2/3}$. The ratios of explicit filter width to grid size are $\overline{\Delta}_k/\Delta_k = 1/\sqrt{3}$, and thus $\overline{\Delta}_{c,k}/\Delta_k = 2$. The basic LES filter (F1) is chosen as ''top hat'' in all directions. We thus have

$$\bar{\mathcal{G}} = \frac{\sin(k_x\Delta_x)}{(k_x\Delta_x)}\,\frac{\sin(k_y\Delta_y)}{(k_y\Delta_y)}\,\frac{\sin(k_z\Delta_z)}{(k_z\Delta_z)}. \tag{39}$$

The dynamic procedure is done with $\alpha = 2$, hence the appropriate test filter is[36]

$$\hat{\mathcal{G}} = \cos(k_x\Delta_x)\cos(k_y\Delta_y)\cos(k_z\Delta_z). \tag{40}$$

This test filter is applied in physical space since, by design, it simply corresponds, in each direction, to the arithmetic mean of the two neighbor grid values (see also Sec. VI).

In order to confirm that it is mostly the normalized filter width that matters (and not much its shape), another explicit filter (F2) was tested: Gaussian in the homogeneous directions (test filter applied in Fourier space) and top hat in the nonhomogeneous direction:

$$\bar{\mathcal{G}} = \exp\left(-\frac{k_x^2\Delta_x^2}{6}\right)\frac{\sin(k_y\Delta_y)}{(k_y\Delta_y)}\exp\left(-\frac{k_z^2\Delta_z^2}{6}\right). \tag{41}$$

It was found that numerical instabilities are generated by the tensor-diffusivity part of the mixed model near the wall: They correspond to long-lived negative diffusion events that eventually make the simulation blow up. As we do not start the LES from filtered and truncated DNS fields, near-wall stability is even more of an issue. To alleviate this problem, damping of the tensor-diffusivity part of the mixed model was used close to the wall, on a scale of the order of the laminar sublayer. We here used, as damping, the simple function $1-\exp(-y^+/c^+)$ with $c^+ = 10$. We acknowledge that such damping is crude and quite arbitrary. More work certainly needs to be done concerning the near-wall stability of the tensor-diffusivity model.

The performance of the mixed model ''so far'' (e.g., with crude damping) is however worth reporting. Results on normalized mean profiles as a function of normalized distance to the wall are provided in Figs. 13 and 14: velocity, model stress, and model dissipation. With the same explicit F1 filtering, the mixed model clearly outperforms the dynamic Smagorinsky model: much better mean velocity profile. Again, we conclude that the partial reconstruction model for the filtered-scale stress is needed. We also see that the velocity profile has the correct slope in the log region. The level is however slightly overpredicted.

The mixed model results obtained using the F2 filter are close to those obtained using F1. This result is comforting: As both filters were normalized the same way, the expectation was that the mixed model would produce similar results. It also confirms that, for LES with explicit filtering, the test filtering can be done in physical space: One only needs to assume that the explicit filter is the top hat with effective width, $\overline{\Delta}_c$, twice the grid size, Δ.

We notice, in Fig. 14, that the contribution of the tensor-diffusivity part of the mixed model is, again, significant; for

Downloaded 10 May 2001 to 128.206.16.97. Redistribution subject to AIP license or copyright, see http://ojps.aip.org/phf/phfcr.jsp

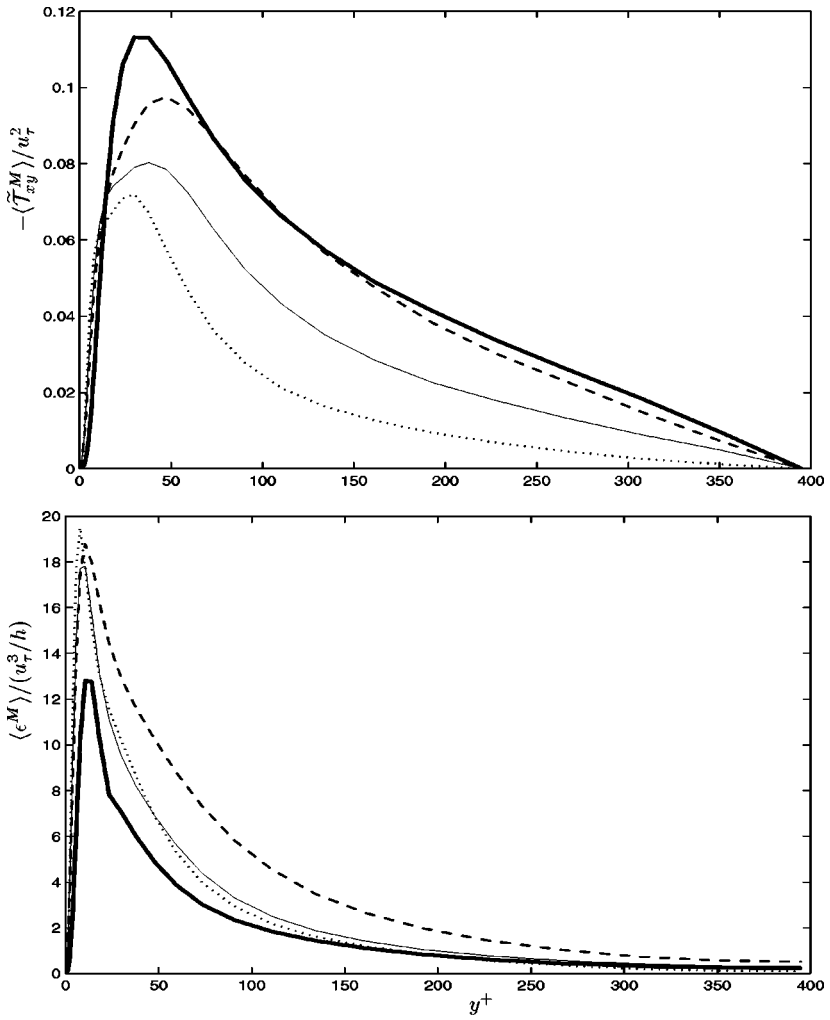

FIG. 14. Mean profiles of model stress and model dissipation: dynamic mixed model, F1: tensor-diffusivity contribution (solid line) and dynamic Smagorinsky contribution (thin solid line); dynamic Smagorinsky model, F1 (dashed line); dynamic Smagorinsky model without explicit filtering, $x-z$ sharp cutoff test filtering (dotted line).

the mean stress, its contribution is slightly higher than that of the dynamic Smagorinsky part; for the mean dissipation, its contribution is slightly lower.

For further comparisons, we also ran the dynamic Smagorinsky model without explicit filtering, using the dynamic procedure with sharp cutoff test filtering in x and z and no test filtering in y: something that is not self-consistent as far as the similarity assumptions underlying the dynamic procedure are concerned (see Sec. VI), but that is nevertheless often used by LES practitioners. The obtained mean velocity profile follows better the DNS data in the transition region, but not in the log region: its slope is too high, see Fig. 13.

We provide, in Fig. 15, the mean stress profile obtained with the mixed model. As expected, the terms add up to the linear profile for the total stress. The main contribution close to the wall is that of the viscous stress. Away from the wall, the main contribution is the *Reynolds* stress of the LES simulation: $-\langle \widetilde{\bar{u}\,\bar{v}} \rangle$ (as $\langle \bar{v} \rangle = 0$). The remainder stress is the model stress $-\langle \widetilde{\mathcal{T}}_{xy}^{M} \rangle$ (with the tensor-diffusivity contribution slightly higher than the Smagorinsky contribution).

The mean dissipation profiles are also provided in Fig. 15. The main contribution close to the wall is that of the viscous stress. Away from the wall, the dominant contribution is that of the model stress (the tensor-diffusivity contribution being slightly lower than the Smagorinsky contribution).

The mean profiles of velocity, model stress, and model dissipation are similar to those obtained by Domaradzki *et al.*[42,43] using their subgrid-scale estimation model.

Based on the usual and good assumption that the average (over time and over the homogeneous directions) of a non-filtered quantity is the same as the average of the filtered quantity, i.e., the assumption that $\langle f \rangle \approx \langle \tilde{f} \rangle \approx \langle \bar{\tilde{f}} \rangle$, it follows that the best reconstruction of the true Reynolds stress (i.e., the one to be compared to the DNS Reynolds stresses) is

$$
\begin{aligned}
R_{ij} &\overset{\text{def}}{=} \langle u_i \rangle \langle u_j \rangle - \langle u_i u_j \rangle \approx \langle \bar{\tilde{u}}_i \rangle \langle \bar{\tilde{u}}_j \rangle - \langle u_i \overline{\widetilde{u_j}} \rangle \\
&= (\langle \bar{\tilde{u}}_i \rangle \langle \bar{\tilde{u}}_j \rangle - \langle \widetilde{\bar{\tilde{u}}_i \bar{\tilde{u}}_j} \rangle) - \langle \widetilde{\mathcal{T}}_{ij} \rangle \\
&\approx (\langle \bar{\tilde{u}}_i \rangle \langle \bar{\tilde{u}}_j \rangle - \langle \widetilde{\bar{\tilde{u}}_i \bar{\tilde{u}}_j} \rangle) - \langle \widetilde{\mathcal{T}}_{ij}^{M} \rangle
\end{aligned}
\tag{42}
$$

and thus that

$$
R_{xy} \approx -\langle \widetilde{\bar{u}\,\bar{v}} \rangle - \langle \widetilde{\mathcal{T}}_{xy}^{M} \rangle. \tag{43}
$$

The combination of the adequate mean stress profiles in Fig. 15 can be compared to the R_{xy} of the DNS: This is done in Fig. 16. The dynamic mixed model again outperforms the

Downloaded 10 May 2001 to 128.206.16.97. Redistribution subject to AIP license or copyright, see http://ojps.aip.org/phf/phfcr.jsp

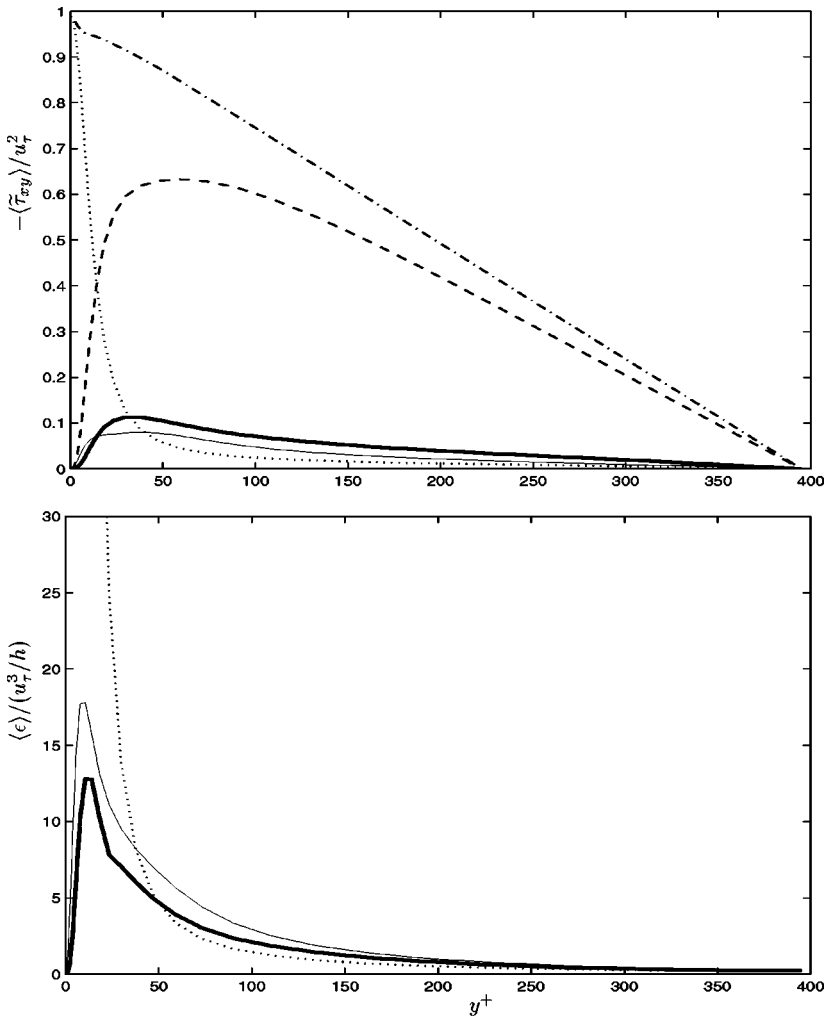

FIG. 15. Mean profiles of stress and dissipation for the dynamic mixed model with F1: tensor-diffusivity contribution (solid line); dynamic Smagorinsky contribution (thin solid line); contribution of $-\langle\widetilde{\bar{u}\,\bar{v}}\rangle/u_\tau^2$ (dashed line); viscous contribution (dotted line); total (chained-dotted line).

dynamic Smagorinsky model. It however produces results similar to those obtained using the dynamic Smagorinsky model without explicit filtering. Even the run without LES modeling produces about the correct R_{xy} profile. R_{xy} does not appear to be a severe diagnostic. Recall also that, when adding the mean viscous stress, one always obtains the linear profile for the total stress, whatever the modeling approach. As to comparison of the diagonal stresses,

$$R_{xx}\approx(\langle\bar{u}\rangle\langle\bar{u}\rangle-\langle\widetilde{\bar{u}\,\bar{u}}\rangle)-\langle\tilde{\mathcal{T}}_{xx}^{M}\rangle, \tag{44}$$

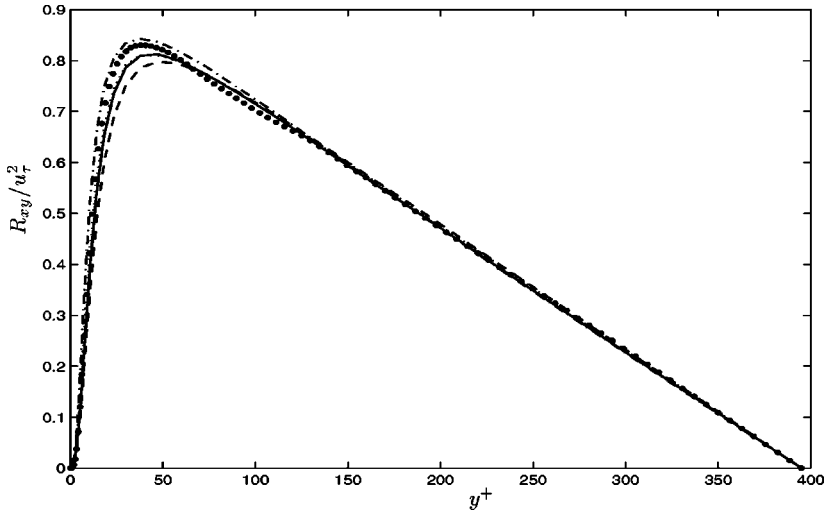

FIG. 16. Profile of the R_{xy} Reynolds stress: DNS (closed circle); dynamic mixed model, F1 (solid line); dynamic Smagorinsky model, F1 (dashed line); dynamic Smagorinsky model without explicit filtering, $x-z$ sharp cutoff test filtering (dotted line); no model (chained-dotted line).

Downloaded 10 May 2001 to 128.206.16.97. Redistribution subject to AIP license or copyright, see http://ojps.aip.org/phf/phfcr.jsp

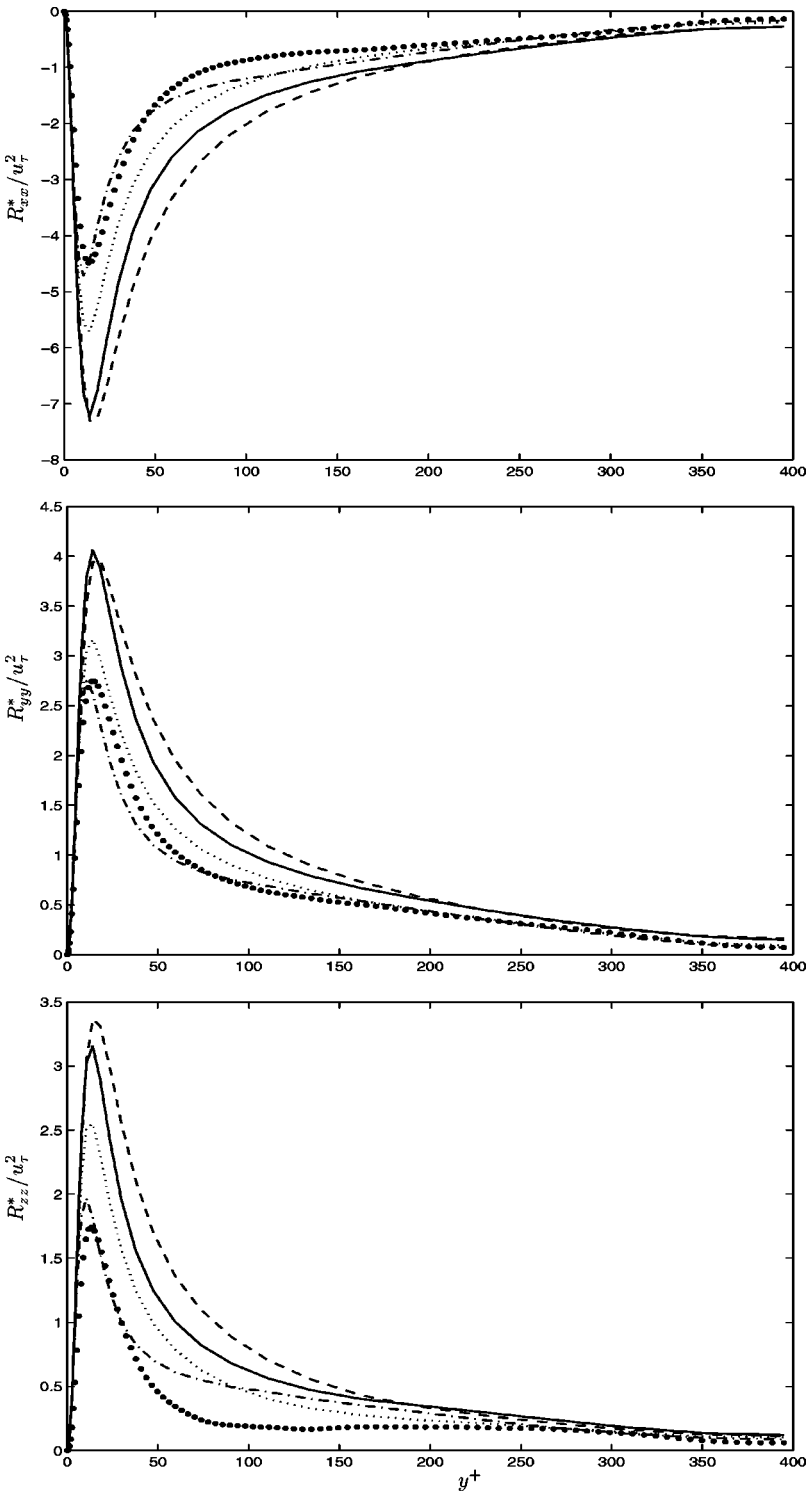

FIG. 17. Profiles of the reduced diagonal Reynolds stresses: DNS (closed circle); dynamic mixed model, F1 (solid line); dynamic Smagorinsky model, F1 (dashed line); dynamic Smagorinsky model without explicit filtering, $x-z$ sharp cutoff test filtering (dotted line); no model (chained-dotted line).

etc., one must be careful: Because of the lack of trace modeling inherent to all effective viscosity truncation models, one can only compare the reduced diagonal stresses: R^*_{xx}, R^*_{yy}, and R^*_{zz}. Thus, one can only compare the deviations from isotropy, see Fig. 17, not the absolute values. This point is important, yet it is often overlooked in the LES literature. The results obtained using the dynamic Smagorinsky model without explicit filtering are seen to be better than those obtained using the dynamic mixed model with damping. Actually, the best results are those obtained without LES modeling. We also notice that the differences with the DNS are systematically more marked for R^*_{xx} and R^*_{zz} than for R^*_{yy}. This might indicate that the LES resolution in x and z is too coarse with respect to capturing the important large structures in the wall region. The DNS has $\Delta_x^+ = 9.7$, $\Delta_z^+ = 6.5$ and $\Delta_{y_c}^+ = 6.5$ (channel center); cutting by a factor of 4 in all directions might simply be too much to ask to the LES in the wall region, whatever the model used (at least as far as R^*_{xx} and R^*_{zz} are concerned).

Downloaded 10 May 2001 to 128.206.16.97. Redistribution subject to AIP license or copyright, see http://ojps.aip.org/phf/phfcr.jsp

IX. CONCLUSIONS

LES with regular explicit filtering (on top of the necessary truncations) was investigated, the filters considered being symmetric and having a nonzero second moment (which is used to define the effective filter width). The tensor-diffusivity model was reviewed: It is generic and corresponds to significant, yet incomplete, reconstruction of the filtered-scale stress. The mixed model, tensor-diffusivity model supplemented by a dynamic Smagorinsky term, was also reviewed, with useful connections to other models. The tensor-diffusivity model was first tested alone, both *a priori* and in actual LES, in turbulent isotropic decay: LES started from a 256^3 DNS at $\mathrm{Re}_\lambda = 90$ that is Gaussian filtered and truncated to 64^3. The model remained stable despite the local directional backscatter, and also produced significant global dissipation: initially, more than half of the amount required for the effective stress (filtered-scale stress+subgrid-scale stress). The mixed model was tested next, with a dynamic procedure formulated and applied in a consistent way. Past the initial transient in the dynamic procedure, the added Smagorinsky term leads to good results—proper dissipation and acceptable energy spectra. The mixed model appears as an efficient model for LES with explicit filtering: a compromise between partial reconstruction of the filtered-scale stress and modeling of the truncation effects (subgrid-scale stress and incomplete reconstruction). The initial spectrum of dissipation was also investigated, illustrating the differences between the terms in the mixed model. The mixed model results (energy decay, energy spectra) were significantly better than those obtained when using the dynamic Smagorinsky model alone, with same explicit filtering: Reconstruction of the filtered-scale stress is necessary. They were also very close to those obtained when using the dynamic Smagorinsky model without explicit filtering. The two approaches were also tested on more challenging 48^3 LES: again, they produced similar results. These findings support the view that the tensor-diffusivity model may well suffice for practical reconstruction of the filtered-scale stress. However, despite the high expectations (also based on favorable *a priori* tests) for LES with explicit filtering and simple mixed modeling, these findings are somewhat disappointing. So far, we conclude that the two modeling approaches lead to similar results in isotropic turbulence. Truncation modeling remains a challenge in LES. In particular, the shortcomings of the Smagorinsky model were seen in both approaches: its inability to properly differentiate between large and small scales.

One question remains: Would the results be significantly improved if we used high level reconstruction of the filtered-scale stress (or, simpler, boost the tensor-diffusivity term by a factor)? This deserves further investigations. Finally, we also retain that, for ''initial value problems'' (here the best possible one: LES started from truncated DNS), the dynamic procedure (here with shift dealiasing and spherical truncation) is found to have initial difficulties in both approaches: C is first overpredicted; it then quickly stabilizes at a proper level. It would also be useful to compare the approaches in forced isotropic turbulence.

The mixed model was also tested on the turbulent channel flow at $\mathrm{Re}_\tau = 395$, using a grid four times coarser than that of the DNS. With the top hat as the assumed explicit filter and the proper filter width, the consistent test filter for the dynamic procedure is easily applied in physical space. Near wall numerical instabilities were observed for the tensor-diffusivity part of the mixed model. In order to alleviate these instabilities, this model part was damped closed to the wall, using simple (and crude) exponential damping. The results obtained so far with the damped mixed model are fair and encouraging. Mean profiles of velocity, stress, dissipation, and reconstructed Reynolds stresses were presented. The dynamic Smagorinsky model for LES without explicit filtering was also run. The mean velocity profile is slightly not as good as that obtained with the damped mixed model, but the reconstructed Reynolds stresses are slightly better.

We retain, for further studies of LES with explicit filtering: (1) the development of better subgrid-scale models (also needed for LES without explicit filtering), (2) the testing of the mixed model in forced isotropic turbulence, (3) the testing of higher level reconstruction of the filtered-scale stress, (4) the better understanding of near-wall stability and the development of better corrections to the tensor-diffusivity part, (5) the effect, in wall proximity, of the coarse longitudinal and transverse spatial resolution (also for LES without explicit filtering), and (6) the possible practical importance of the y-grid nonuniformity on the modeling (possible significant commutation errors for grids that are nonuniform,[44] yet have a smooth variation). Finally, the development of approximate wall proximity boundary conditions to allow for LES without resolving the wall region remains a subject of high interest. Here, it could also eliminate the near wall stability problem of the mixed model.

ACKNOWLEDGMENTS

Some preliminary work started during the CTR Summer Program 1998.[1] It was further improved, corrected, and enlarged, also with support of the *Fonds de la Recherche Fondamentale Collective*, Belgium (convention FRFC 2.4563.98), to produce this paper. We also thank F. Thirifay for his help in producing figures.

[1] G. S. Winckelmans, A. A. Wray, and O. V. Vasilyev, ''Testing of a new mixed model for LES: The Leonard model supplemented by a dynamic Smagorinsky term,'' Proceedings of the Summer Program, Center for Turbulence Research, Stanford University and NASA Ames, 1998, pp. 367–388.

[2] A. Leonard and G. S. Winckelmans, ''A tensor-diffusivity subgrid model for largeeddy simulation,'' Proceedings of the Isaac Newton Institute Symposium / ERCOFTAC Workshop, Cambridge, UK, 12–14 May 1999, *ERCOFTAC Series: Direct and Large-Eddy Simulation III*, edited by P. R. Voke, N. D. Sandham, and L. Kleiser (Kluwer Academic, Dordrecht, 1999), pp. 147–162.

[3] A. Leonard, ''Energy cascade in large-eddy simulations of turbulent fluid flows,'' Adv. Geophys. **18**, 237 (1974).

[4] B. Vreman, B. Geurts, and H. Kuerten, ''Large-eddy simulation of the temporal mixing layer using the mixed Clark model,'' Theor. Comput. Fluid Dyn. **8**, 309 (1996).

[5] B. Vreman, B. Geurts, and H. Kuerten, ''Large-eddy simulation of the turbulent mixing layer,'' J. Fluid Mech. **339**, 357 (1997).

[6] D. Carati, G. S. Winckelmans, and H. Jeanmart, ''On the modeling of the subgrid-scale and filtered-scale stress tensors in large-eddy simulation,'' to appear in J. Fluid Mech.

Downloaded 10 May 2001 to 128.206.16.97. Redistribution subject to AIP license or copyright, see http://ojps.aip.org/phf/phfcr.jsp

[7]W. K. Yeo, ''A generalized high pass/low pass filtering procedure for deriving and solving turbulent flow equations,'' Ph.D. thesis, Ohio State University, 1987.
[8]W. K. Yeo and K. W. Bedford, ''Closure-free turbulence modeling based upon a conjuctive higher order averaging procedure,'' in *Computational Methods in Flow Analysis*, edited by H. Niki and M. Kawahara (Okayama University of Science, Okayama, 1988), pp. 844–851.
[9]K. W. Bedford and W. K. Yeo, ''Conjunctive filtering procedures in surface water flow and transport,'' in *Large Eddy Simulation of Complex Engineering and Geophysical Flows*, edited by B. Galperin and S. A. Orszag (Cambridge University Press, Cambridge, 1993), pp. 513–537.
[10]A. Leonard, ''Large-eddy simulation of chaotic convection and beyond,'' *35th Aerospaces Sciences Meeting & Exhibit*, Reno, NV, 6–10 January, 1997, AIAA Paper No. 97-0204.
[11]D. Carati, G. S. Winckelmans, and H. Jeanmart, ''Exact expansions for filtered-scales modelling with a wide class of LES filters,'' in Ref. 2, pp. 213–224.
[12]S. Stolz and N. A. Adams, ''An approximate deconvolution procedure for large-eddy simulation,'' Phys. Fluids **11**, 1699 (1999).
[13]S. Liu, C. Meneveau, and J. Katz, ''On the properties of similarity subgrid-scale models as deduced from measurements in a turbulent jet,'' J. Fluid Mech. **275**, 83 (1994).
[14]V. Borue and A. Orszag, ''Local energy flux and subgrid-scale statistics in three-dimensional turbulence,'' J. Fluid Mech. **366**, 1 (1998).
[15]J. Smagorinsky, ''General circulation experiments with the primitive equations,'' Mon. Weather Rev. **91**, 99 (1963).
[16]M. Germano, U. Piomelli, P. Moin, and W. Cabot, ''A dynamic subgrid-scale eddy-viscosity model,'' Phys. Fluids A **3**, 1760 (1991).
[17]S. Ghosal, T. S. Lund, and P. Moin, ''A local dynamic model for large-eddy simulation,'' in Annual Research Briefs, Center for Turbulence Research, Stanford University and NASA Ames, 1992, pp. 3–25.
[18]P. Moin, D. Carati, T. Lund, S. Ghosal, and K. Akselvoll, ''Developments and applications of dynamic models for large eddy simulation of complex flows,'' Proceedings of the 74th Fluid Dynamics Symposium on Application of Direct and Large Eddy Simulation to Transition and Turbulence, Chania, Crete, Greece, 1994, AGARD-CP-551, 1-1-9.
[19]S. Ghosal, T. S. Lund, P. Moin, and K. Akselvoll, ''A dynamic localization model for large-eddy simulation of turbulent flows,'' J. Fluid Mech. **286**, 229 (1995).
[20]D. Carati, S. Ghosal, and P. Moin, ''On the representation of backscatter in dynamic localization models,'' Phys. Fluids **7**, 606 (1995).
[21]N. N. Mansour, J. H. Ferziger, and W. C. Reynolds, ''Large-eddy simulation of a turbulent mixing layer,'' Thermosciences Div., Mech. Eng. Dept., Stanford University, Report No. TF-11, 1978.
[22]R. A. Clark, J. H. Ferziger, and W. C. Reynolds, ''Evaluation of subgrid-scale models using a fully simulated turbulent flow,'' Thermosciences Div., Mech. Eng. Dept., Stanford University, Report No. TF-9, 1977.
[23]R. A. Clark, J. H. Ferziger, and W. C. Reynolds, ''Evaluation of subgrid-scale turbulence models using an accurately simulated turbulent flow,'' J. Fluid Mech. **91**, 1 (1979).
[24]G. S. Winckelmans, T. S. Lund, D. Carati, and A. A. Wray, ''*A priori* testing of subgrid-scale models in the velocity-pressure and the vorticity-velocity formulations,'' Proceedings of the Summer Program, Center for Turbulence Research, Stanford University and NASA Ames, 1996, pp. 309–328.
[25]D. Carati, K. Jansen, and T. Lund, ''A family of dynamic models for large-eddy simulation,'' in Annual Res. Briefs, Center for Turbulence Research, Stanford University and NASA Ames, 1995, pp. 35–40.
[26]G. Dantinne, H. Jeanmart, G. S. Winckelmans, V. Legat, and D. Carati, ''Hyperviscosity and vorticity-based models for subgrid scale modeling,'' Appl. Sci. Res. **59**, 409 (1998).
[27]F. Nicoud and F. Ducros, ''Subgrid-scale stress modeling based on the square of the velocity gradient tensor,'' Flow, Turbul. Combust. **62**, 183 (1999).
[28]D. Carati and W. Cabot, ''Anisotropic eddy viscosity models,'' Proceedings of the Summer Program, Center for Turbulence Research, Stanford University and NASA Ames, 1996, pp. 249–258.
[29]T. J. R. Hughes, L. Mazzei, A. A. Oberai, and A. A. Wray, ''The multiscale formulation of large eddy simulation: Decay of homogeneous isotropic turbulence,'' Phys. Fluids. **13**, 505 (2001).
[30]T. S. Lund and E. A. Novikov, ''Parametrization of subgrid-scale stress by the velocity gradient tensor,'' in Annual Research Briefs, Center for Turbulence Research, Stanford University and NASA Ames, 1992, pp. 27–43.
[31]J. Bardina, J. H. Ferziger, and W. C. Reynolds, ''Improved turbulence models based on large eddy simulation of homogeneous incompressible turbulence,'' Thermosciences Div., Mech. Eng. Dept., Stanford University, Report No. TF-19, 1983.
[32]K. Horiuti, ''A new dynamic two-parameter mixed model for large-eddy simulation,'' Phys. Fluids **9**, 3443 (1997).
[33]G.-H. Cottet and A. A. Wray, ''Anisotropic grid-based formulas for subgrid-scale models,'' in Annual Research Briefs, Center for Turbulence Research, Stanford University and NASA Ames, 1997, pp. 113–122.
[34]G.-H. Cottet and O. V. Vasilyev, ''Comparison of dynamic Smagorinsky and anisotropic subgrid-scale models,'' Proceedings of the Summer Program, Center for Turbulence Research, Stanford University and NASA Ames, 1998, pp. 367–388.
[35]G.-H. Cottet, ''Artificial viscosity models for vortex and particle methods,'' J. Comput. Phys. **127**, 299 (1996).
[36]D. Carati and E. Vanden Einden, ''On the self-similarity assumption in dynamic models for large eddy simulations,'' Phys. Fluids **9**, 2165 (1997).
[37]B. J. Geurts, ''Balancing errors in LES,'' in Ref. 2, pp. 1–12.
[38]Y. Morinishi, T. S. Lund, O. V. Vasilyev, and P. Moin, ''Fully conservative higher order finite difference schemes for incompressible flow,'' J. Comput. Phys. **143**, 90 (1998).
[39]O. V. Vasilyev, ''High order finite difference schemes on non-uniform meshes with good conservation properties,'' J. Comput. Phys. **157**, 746 (2000).
[40]N. N. Mansour, R. D. Moser, and J. Kim, ''Reynolds number effects in low Reynolds number turbulent channel,'' data in AGARD database, 1996.
[41]R. D. Moser, J. Kim, and N. N. Mansour, ''Direct numerical simulation of turbulent channel flow up to Re_τ=590,'' Phys. Fluids **11**, 943 (1999).
[42]J. A. Domaradzki and E. M. Saiki, ''A subgrid-scale model based on the estimation of unresolved scales of turbulence,'' Phys. Fluids **9**, 2148 (1997).
[43]J. A. Domaradzki and K.-C. Loh, ''The subgrid-scale estimation model in the physical space representation,'' Phys. Fluids **11**, 2330 (1999).
[44]S. Ghosal and P. Moin, ''The basic equations for the large-eddy simulation of turbulent flows in complex geometry,'' J. Comput. Phys. **118**, 24 (1995).

Downloaded 10 May 2001 to 128.206.16.97. Redistribution subject to AIP license or copyright, see http://ojps.aip.org/phf/phfcr.jsp